Studies on Electrochemical Properties of Alkanethiol Self-Assembled Monolayers and Their Application for Fabrication of Nano-Structured Electrodes

（アルカンチオール自己集合単分子膜の電気化学的評価とナノ構造電極の構築への応用）

2004

HIROKAZU MUNAKATA

Department of Materials Chemistry
Graduate School of Engineering
Osaka University

Preface

The work of this thesis was carried out under the guidance of Professor Dr. Susumu Kuwabata at Department of Materials Chemistry, Graduate School of Engineering, Osaka University.

The objects of this thesis are to investigate electrochemical properties of a self-assembled monolayer of alkanethiols and to develop them for novel preparation of nano-structured electrode surfaces. Recently, special attention has been paid in various fields to fabrication of sophisticated structures by self-assembly. The author hopes that the knowledge obtained in this work would contribute to progress of electrochemistry of self-assembled complex systems and nano technology.

Hirokazu Munakata

Department of Materials Chemistry
Graduate School of Engineering
Osaka University
Yamada-oka 2-1, Suita, Osaka 565-0871, Japan

March / 2004

Contents

General Introduction

Background

Organosulfur compounds such as alkanethiols, dialkyl disulfides, and dialkyl sulfides chemisorb on metal surfaces and form spontaneously a highly ordered monolayer, which is widely called a self-assembled monolayer (SAM). This interesting phenomenon has been first reported by Allara and Nuzzo at Bell laboratories in 1983.[1] Unlike a Langmuir-Blodgett (LB) film,[2,3] the SAM has strong adhesion to substrates, high degree of thermal and chemical stabilities, and mechanical strength. In addition, ease of preparation of such the stable monolayer with high reproducibility allows investigation of the monolayer properties. Then, thiol-SAMs has been studied extensively as a new method to provide well defined structural interfaces.[4-6]

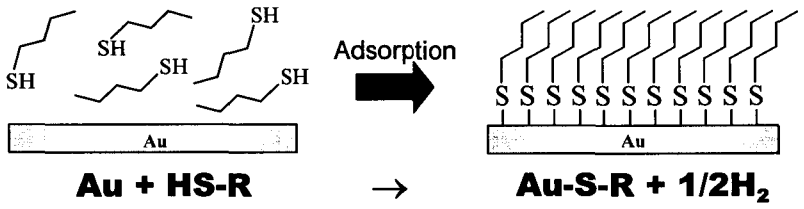

Self-assembly of alkanethiols on Au substrate.

Since alkanethiols substituted by functional groups at ω-position are available, one can introduce desired properties on metal surfaces.[7-10] For example, wetting control[11,12] and corrosion protection of the surfaces[13] were reported. In addition, SAMs composed of two or more kinds of thiols prepared by coadsorption are frequently utilized for tailoring desired surface structures in molecular order.[14-25] Whitesides and coworkers, who developed a method preparing binary component SAMs by coadsorption, provides that changes in composition of SAM formed on an Au substrate allowed gradual transition of surface properties, and they acquired considerable

information on the physical and chemical properties of the binary SAMs with the use of surface measurement techniques.[9-12,26-33]

To elucidate properties of the SAMs, various techniques have been employed, including ellipsometry,[7] XPS,[10] contact angle measurements,[21] quartz crystal microbalance,[34-37] and so on. Especially, recent improvements of scanning tunneling microscopy (STM) and atomic force microscopy (AFM) have made it possible to observe the surface structures in atomic resolution and allow us to investigate the relationship between assembled structures of SAMs and their resulted properties.[38,39] Porter et al. found that desorption of alkanethiol-SAMs on Au and Ag surfaces can be conducted by electrochemical means.[40,41] The reduction waves for desorption measured by conventional voltammetry provide a sensitive indication of the condition of SAMs such as the length of alkyl chain or surface coverage. Then, this method is widely utilized for characterizing the thiol-SAMs.

The Present Work

The present study has been conducted focusing on elucidation of the mechanism of reductive desorption of the alkanethiol-SAMs, and its application to a novel method to evaluate interfacial properties on SAMs or fabrication of nano-structured electrode surfaces. This thesis consists of four chapters.

In chapter 1, it is described a novel method to detect surface acidities of functional groups induced specifically by arrayed groups in monolayers, by using desorption of thiol-SAMs measured by conventional voltammetry. In chapter 2, the SAM-desorption technique has been extended to investigate electrochemical properties of ions on interfacial properties between ionic liquids and SAMs. Chapter 3 deals with bilayer membrane composed of lipid monolayer and SAM of alkanethiol on a metal substrate. Here it is discussed that this bilayer membrane is useful for studies on dynamic relocation of lipid molecules in the bilayer membrane, and the electrochemical methods to evaluate fluidity of lipid membrane and formation rate of the bilayer membrane by fusion of the liposome have been developed. In chapter 4 it is discussed the

preparation and characterization of nano-structured electrode surfaces with use of binary SAMs induced by selective desorption. The parameters influenced the form or spatial distribution of nano-structures, such as degree of difference in the lengths of thiols composing the binary SAMs, are discussed in detail.

Chapter 1

Effect of ω-Functional Groups on pH-Depended Reductive Desorption of Alkanethiol Self-Assembled Monolayers

1-1. Introduction

Monolayers composed of closely packed organic species are of great interest as models of biomembranes. In particular, monolayers containing acidic or basic groups are useful for understanding roles of those species in various functions of cell membranes, such as cell fusion, enzymatic catalysis, and ion transfer. One of the well known specific properties of closely packed groups is that acidities of groups like carboxyl and amino are different from their original values. Such behavior has been first found by potentiometric titration of micellar solutions of various surfactants.[42-46]

A SAM of alkanethiols adsorbed on a gold surface provides another monolayer system and is an ideal model for understanding properties of solid surfaces. In this case also, determination of acidity of arrayed groups is currently attracting great attention. To detect properties of the delicate monolayer surfaces special techniques such as contact angle titration,[21] quartz crystal microbalance,[34-37] capacitance measurement,[47-49] interfacial force and probe spectroscopy,[50-53] must be adopted. In some cases, the help of difficult theory and calculations is needed to determine the desired parameters.

In this chapter, I would like to show that electrochemical desorption reaction of a thiol SAM measured by conventional voltammetry becomes a useful method for investigating the delicate properties of SAMs. In particular, the desorption reaction of thiol molecules having carboxyl and amino terminals have been thoroughly examined as a method to evaluate pK_a values of these terminal groups.

1-2. Experimental Section

Materials. *n*-Alkanethiols terminated by methyl group [HS-$(CH_2)_n$-CH_3 with n = 1, 2, 7, 9 (Wako Pure Chemicals)], hydroxyl group [HS-$(CH_2)_n$-OH with n = 2, 4 (Wako Pure Chemicals), and 6, 8 (Dojindo Laboratories)], carboxyl group [HS-$(CH_2)_n$-COOH with n = 2, 5, 7, 10 (Dojindo Laboratories)], and amino group [HS-$(CH_2)_n$-NH_2 with n = 2, 8, 11 (Dojindo Laboratories)] were reagent grade chemicals and were used without specific purification. Water used for preparation of electrolyte solution was purified by a Milli-Q Gradient A10 (ρ > 18.2 MΩcm). All other chemicals were of reagent grade.

An electrode substrate used in this study was prepared by vacuum evaporation of an Au (300 nm thickness) on a freshly cleaved natural mica sheet, which was heated at 300 °C more than 2 h prior to the evaporation and during the Au deposition. Pressure chosen was below 5 × 10^{-6} Torr. It was confined by observation with a scanning tunneling microscopy that the obtained Au electrode has atomically flat (111) terraces. Formation of a thiol SAM was made by immersing the Au substrate for 1 h in an ethanol solution containing one of the above-mentioned thiols in 1 mmol dm^{-3}. The prepared electrode was then rinsed with ethanol and water.

Methods. Electrochemical experiments were carried out using a glass tube cell whose ends were open. The SAM-coated Au electrode was attached at the bottom hole of the cell with a Teflon-coated O-ring to give an active electrode area of 0.40 ± 0.02 cm^2, which was estimated by measuring the charges involved in oxidation of chemically adsorbed iodine.[54-56] After pouring electrolyte solution, the cell was capped with a silicon rubber equipped with a reference electrode of Ag|AgCl in KCl-saturated aqueous solution and a Pt foil counter electrode. Measurements were made by an ALS-701 electrochemical analyzer. The electrolyte solution used for electrochemical desorption of thiols was deaerated by bubbling nitrogen gas for 15 min at least prior to the desorption experiments. The software equipped in the ALS electrochemical analyzer possessed a function capable of integration of redox waves appeared in the obtained voltammograms, allowing electrochemical estimation of the amount of thiol molecules adsorbed

on the Au electrode under an assumption that the reductive desorption of thiol is induced by one electron reaction.

1-3. Results and Discussion

1-3-1. OH-terminated thiol SAM

Figure 1-1 shows linear sweep voltammograms of 2-mercaptoethanol (2-ME) SAM-coated Au(111) electrodes taken at a scan rate of 200 mVs^{-1} in 0.1 mol dm^{-3} phosphate buffer solutions having different pH from 4.53 to 11.49. Cathodic waves representing reductive desorption of thiol appeared in all cases and the peak potential was positively shifted with decreasing pH of the electrolyte solution. It is also recognized that the decrease in pH induced broadening of the wave and lowering of its height. Although such the changes in shape of the wave occurred, the charges calculated by integration of cathodic currents gave almost the same value of (8.0 ± 0.4) x 10^{-5} C

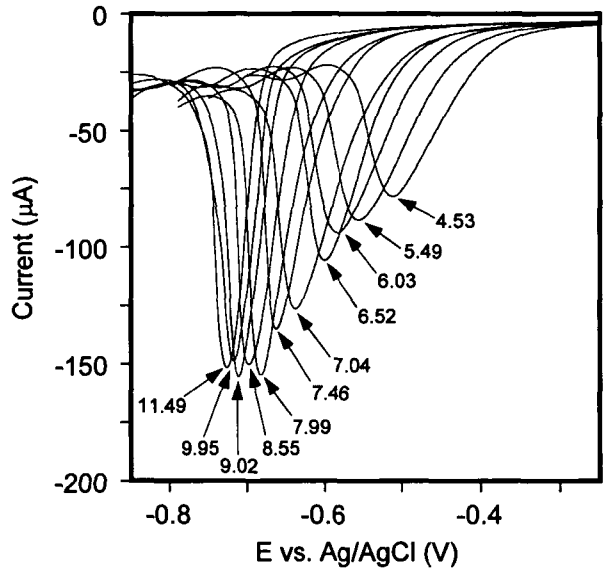

Figure 1-1. Linear sweep voltammograms of 2-mercaptoethanol SAMs on Au(111) electrodes taken at 200 mVs^{-1} in 0.1 mol dm^{-3} phosphate buffer having given pH values.

cm^{-2}, which corresponded to $(8.3 \pm 0.4) \times 10^{-10}$ mol cm^{-2} of amount of 2-ME adsorbed on the electrode. It is well known that thiol molecules closely packed in a SAM are arrayed on Au(111) with the $(\sqrt{3} \times \sqrt{3})R30°$ structure, giving a molecular density of 7.6×10^{-10} mol cm^{-2}.[40] The fact that the experimentally obtained values were close to this value suggested the 2-ME SAM kept the packed structure in the solutions of different pH just before the electrochemical reduction.

In order to clarify the dependency of the cathodic wave on solution pH, the peak potentials (E_p) and full-widths at half-maximum (FWHM) of the waves are plotted as a function of pH, as shown in Figure 1-2 (a) and (b), respectively. In many other studies, the reductive desorption of an alkanethiol-SAM was usually made in strong alkaline solutions because it is expected that the thiolate ions are completely dissolved in solution after desorption from the electrodes.[40,41,57-59] Then, the reaction can be formulated by

$$\text{Au-S-R} + e^- \rightarrow \text{Au} + {}^-\text{S-R} \qquad (1)$$

where R denotes an alkyl group. However, if the solution pH is larger than pK_a value of thiol group, protonation should be accompanied with the desorption reaction. Thus, the reaction can be given by eq. (2).

$$\text{Au-S-R} + e^- + H^+ \rightarrow \text{Au} + \text{HS-R} \qquad (2)$$

The Nernst equation predicts that the redox potential of eq. (2) is shifted by pH changes with a slope of -59 mV / pH. Figure 1-2(a) shows that shift of the E_p with a slope of -55 mV / pH at pH < pK_a of thiol group of 2-ME (9.5).[60] Then, the obtained results seem to reflect well the above-mentioned two reactions although the E_p of the desorption wave is not directly related to the redox potential.

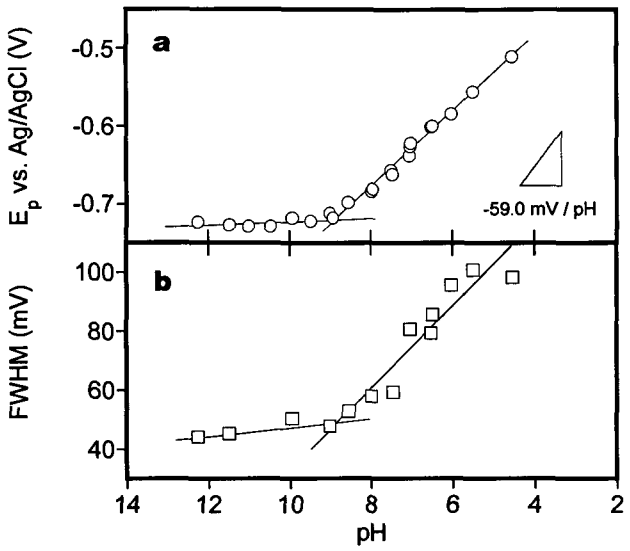

Figure 1-2. Plots of peak potentials (a) and FWHM (b) of cathodic waves due to reductive desorption of 2-ME SAMs as a function of pH of electrolyte solution.

Changes in shape of the cathodic wave representing desorption of SAM have been investigated by some research groups.[61-63] It is then recognized that the length of alkyl chain of alkanethiol-SAM is a dominant factor influencing the shape of the voltammogram. For example, short alkanethiol-SAM gives a single sharp wave, but the wave tends to have a shoulder and ultimately splits into separate peaks as the alkyl chains become longer.[62] Spectroelectrochemical measurements of the SAM desorption have revealed residence of alkanethiol molecules having different orientation of the alkyl chain on the electrode surface during the course of reductive desorption.[63] Based on such the information, the following discussion has been made. Since long alkanethiol molecules have low solubility in aqueous solution, they tend to stay on the electrode surface after the reductive desorption, resulting in formation of some different states of the molecules including randomly physisorbed species and physisorbed micelles. Accordingly, presence of different desorption products would give different electrochemical processes having different redox potentials. Hence, the above-mentioned changes in the shape of the voltammograms are induced. It is likely that similar deduction can be made to explain the broadening of the desorption wave of 2-ME with decreasing pH, as shown in Figure 1-1. It is

noted from the plots of FWHM shown in Figure 1-2(b) that the broadening occurred when solution pH was smaller than pK_a of 2-ME. In this pH region, both negatively charged thiolate and neutral thiol are products of the desorption reaction and ratio of the latter species increases with a decrease in pH. Therefore, increase in production of the thiol molecules having lower solubility seems to increase number of the electrochemical processes, resulting in the broadening of the desorption wave.

Figure 1-3 shows plots of the E_p obtained for desorption of three different OH-terminated thiol SAMs having alkyl chains ($HS-(CH_2)_n-OH$ with n = 4, 6, 8) as a function of pH of electrolyte solution. As the alkyl chain of thiols became longer, E_p shifted to negative potential. Similar relationship has been already reported for other kinds of thiol-SAM.[59] In the SAM, alkyl groups of alkanethiol molecules tug at one another due to the intermolecular forces, which gives the densely packed monolayer. The forces increase with an increase in length of the alkyl groups. Since it is needed to apply excess energy for the reductive desorption of the SAM accompanied with breaking the firmly assembled molecules, over potentials required for inducing the reaction should become larger with increasing alkyl chain length, causing the negative shifts of E_p.

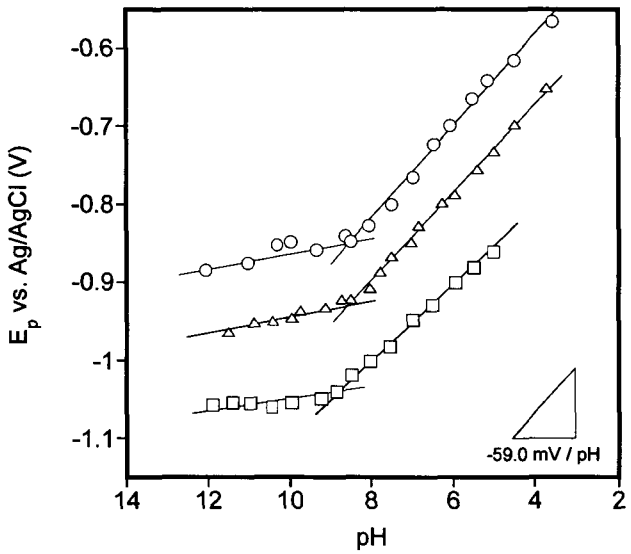

Figure 1-3. Plots of peak potentials of cathodic waves due to reductive desorption of OH-terminated alkanethiol SAMs of n = 4 (○), 6 (Δ), and 8(□) as a function of pH of electrolyte solution. Voltammograms were measured at 200 mVs^{-1} in 0.1 mol dm^{-3} phosphate buffer.

However, it is the fact found first in this study that the relationship between E_p and length of alkyl chain is kept with the same ratio, regardless of solution pH. In the case of SAM of $HS-(CH_2)_n-OH$, -51 mV / n was estimated.

1-3-2. CH_3-terminated thiol SAM

Figure 1-4 shows plots of E_p resulted from reductive desorption of normal CH_3-terminated alkanethiols having various length of alkyl chain ($HS-(CH_2)_n-CH_3$ with n = 1, 2, 7, 9) as a function of pH of electrolyte solution. In the same manner as the case of OH-terminated thiol SAM, there are two pH regions are recognized: pH-independent region and linear change region. The pH value of 10 where the bending point is observed agrees well with pK_a of thiol group in a methyl-terminated alkanethiol, which is slightly larger than that of OH-terminated one (e.g. the pK_a of an ethanethiol is 10.5[60]). It is, therefore, suggested that desorption of CH_3-terminated SAMs also proceeds according to the reactions of eq. (1) and eq. (2) in the solution of pH > pK_a and pH < pK_a, respectively. However, the slope of E_p at pH < pK_a was estimated to be -33 mV, which was apparently much smaller than the slope expected from the Nernst equation.

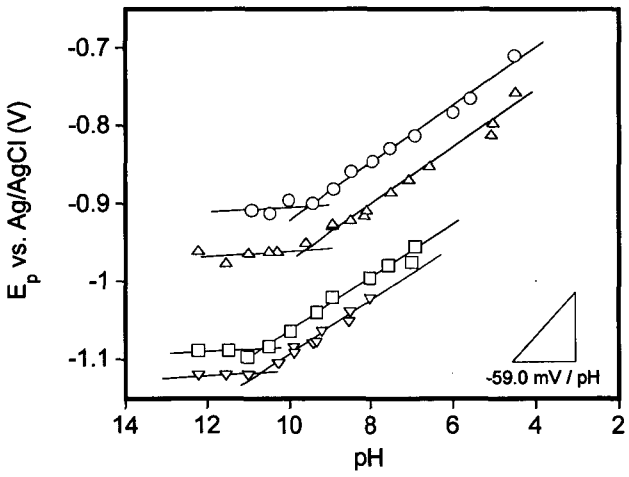

Figure 1-4. Plots of peak potentials of cathodic waves due to reductive desorption of CH_3-terminated alkanethiol SAMs of n = 1 (○), 2 (Δ), 7(□), and 9(▽) as a function of pH of electrolyte solution. Voltammograms were measured at 200 mVs^{-1} in 0.1 mol dm^{-3} phosphate buffer.

The desorption of alkanethiol-SAM with the eq. (1) in strong alkaline solution requires charge compensation by electrolyte cations for generated thiolate anions. In an initial stage of the reaction, since thiolate anions generate at the interior of the monolayer, cations must penetrate through the packed alkyl layer. Therefore, properties of electrolyte cations must influence the desorption behavior of alkanethiol-SAM, and validity of this assumption has been clarified by voltammetry studies on desorption of SAM with changes in kinds of electrolyte cations and their concentrations.[40] Comparison of results shown in Figure 1-4 with those shown in Figure 1-2(a) allows to recognize importance of surface properties of SAM for its desorption. If E_p values obtained in the pH-independent region for OH-terminated thiol SAM and CH_3-terminated one having the same length are compared, the former SAM is apparently desorbed at more positive potentials. This seems to be understood by consideration of hydrophilicity of the terminal groups. It should be easier for electrolyte cations to approach and go into the monolayer having hydrophilic OH groups on its surface than the completely hydrophobic monolayer. Then, decrease in the blocking effects of SAM results in positive shift of the reduction wave.

In the case of the reductive desorption in the pH region where linear change in E_p is observed, protons as well as electrolyte cations are included in the reaction and ratio of contribution of the both species to the reaction depends on H^+ activity in solution. As mentioned above, in an initial stage of the desorption, species presenting in electrolyte solution have to penetrate the monolayer for compensating charges of the generated thiolate anions. This must be true at $pH < pK_a$ not only for electrolyte cation but also for H^+ and water. If the environment around the thiolate groups became the same as electrolyte solution soon after initiation of the desorption reaction, potential shift of E_p would be almost dependent on H^+ activity in the electrolyte solution. The desorption behavior of the OH-terminated SAM might be this case. It is, however, unlikely that the hydrophobic CH_3-terminated SAM allows easily all species in aqueous solution to penetrate through the monolayer even after initiation of the desorption reaction. Therefore, H^+ activity around the generated thiolate anions might not be directly reflected by that of the electrolyte solution, giving the slope of linear changes in E_p that is much smaller than the expected value.

1-3-3. COOH-terminated thiol SAM

Figure 1-5 shows relationships between E_p and pH obtained for COOH-terminated alkanethiol SAMs. All SAMs except for the 11-mercaptoundecanoic acid (n = 10) SAM exhibit two distinct bending points. In the case of 3-mercaptopropionic acid (MPA, n = 2) SAM, the bending points appear at pH = 4.3 and 7.5. At the regions of pH < 4.3 and 7.5 < pH, linear relations were observed and the same slope of -50 mV / pH was estimated. If the eq. (2) occurs, the experimentally obtained slope was a little smaller than that expected from the Nernst equation. Since protons in the electrolyte solution need to penetrate through the closely packed alkyl chains of the thiols in the case of the reductive desorption of the thiol-SAM, the kinetic factors mentioned in previous section seem to be the cause of differences between the experimentally obtained slope and the theoretical one.

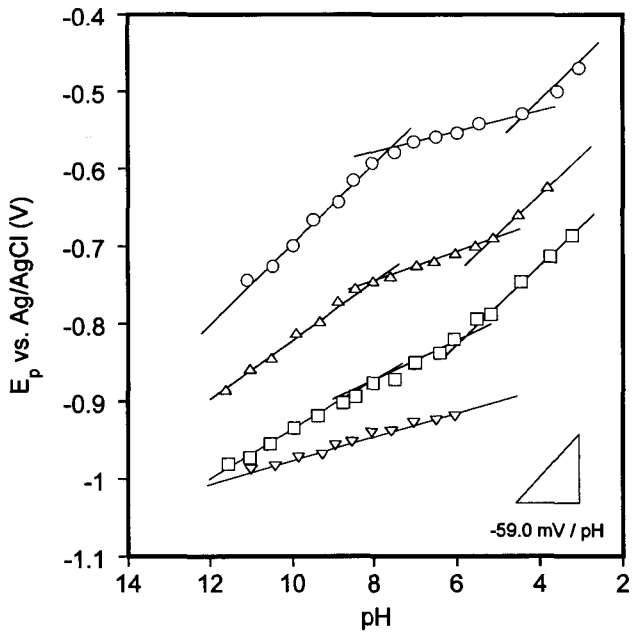

Figure 1-5. Plots of peak potentials of cathodic waves due to reductive desorption of COOH-terminated alkanethiol SAMs of n = 2 (○), 5 (Δ), 7(□), and 10(▽) as a function of pH of electrolyte solution. Voltammograms were measured at 200 mVs^{-1} in 0.1 mol dm^{-3} phosphate buffer.

The finding that one of the bending points appeared at pH = 4.3 coincident with the pK_a value of carboxyl group of MPA,[60] indicates that R in eq. (2) should be $(CH_2)_2$-COOH and $(CH_2)_2$-COO^- at the regions of pH < 4.3 and 7.5 < pH, respectively. However, a small pH dependence of -10 mV / pH was observed at 4.3 < pH < 7.5. As mentioned in the introductory remarks, closely arrayed carboxyl groups posses pK_a values that differ from the original. In the case of the MPA-SAM on Au(111) electrode, values ranging from 5.8 to 8 were evaluated by quartz crystal microbalance measurements,[34-37] AC impedance,[47-49] and atomic force microscopy.[50-53] If such a phenomenon is considered, one can image that there is a pH region where carboxyl groups in MPA-SAM are protonated but deprotonated in the solution. By combining this idea with reductive desorption reaction given eq. (2), the reaction given in eq. (3) is appropriate at that pH region.

$$Au\text{-}S\text{-}(CH_2)_2\text{-}COOH + e^- \rightarrow Au + HS\text{-}(CH_2)_2\text{-}COO^- \qquad (3)$$

The deprotonation of the carboxyl group and protonation of the generated thiolate take place simultaneously, resulting in the exclusion of protons from reaction. The reaction having lower pH dependence observed at 4.3 < pH < 7.5 is attributable to the reaction given by eq. (3) and pH = 7.5 where another bending point appeared can be regarded as the pK_a value of the carboxyl groups in MPA-SAM. However, although the eq. (3) predicts null pH-dependence of the reaction in this pH region, a slope around -10 mV / pH was observed and the slope was increased as length of thiol was longer. In the case of the CH_3-terminated SAM, it was speculated that kinetic factors including penetration of species in the electrolyte solution through the monolayer were reasons giving the pH-dependence smaller than the expected one. Similar factors seem to give some slopes for the pH dependence of E_p due to the reaction (3) as judged from the results shown in Figure 1-6 indicating the titration profiles of E_p taken at different potential sweep rates. Apparently slowing of the potential sweep made the slope of E_p at 4.3 < pH < 7.5 smaller without any shift of locations of the both bending points. The slope of -4 mV / pH was observed for measurements at 10 mVs^{-1}. If relatively high sweep rates were chosen for

the voltammetry measurements, the electrode potential would change at a rate higher than the rate of penetration of H^+ through MPA-SAM. It is, then, supposed that the peaks of the cathodic waves do not appear at potentials that are expected from pH of the electrolyte solution.

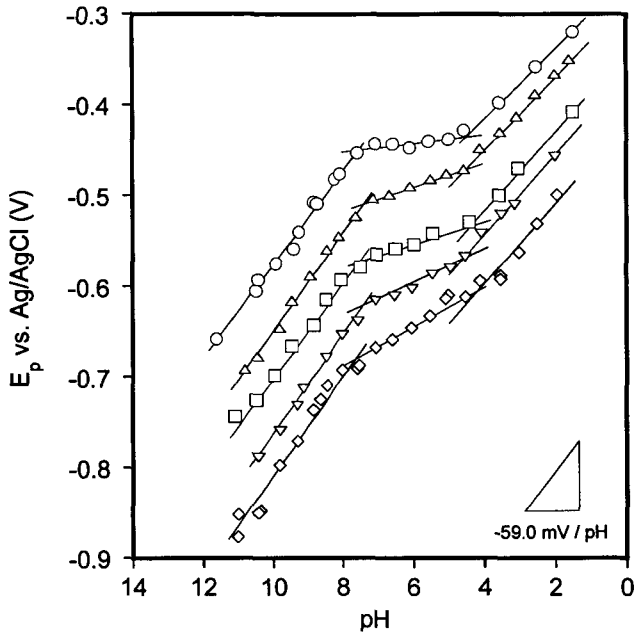

Figure 1-6. Titration curves obtained from peak potentials of cathodic waves due to reductive desorption of COOH-terminated alkanethiol SAM with n = 2 taken at 10 (○), 50 (Δ), 200(□), 500(▽), and 1000 (◇) mVs^{-1}.

1-3-4. NH_2-terminated thiol SAM

To extend applicability of the SAM-desorption technique for evaluating the surface acidity, the titration curves for alkanethiols having amino groups were investigated and obtained results are shown in Figure 1-7. All titration curves indicate two distinct bending points at pH = 6.4 - 6.8 and pH = 8.6 - 8.9. The latter values agree well with pK_a values of primary alkylamines. Then, linear change in E_p observed at pH > 8.9 is attributable to the reaction (2) where R is $(CH_2)_n$-NH_2. However, the observed slopes around -30 mV / pH were smaller than the ideal value although the

hydrophilic amino groups exposed on the surface of the monolayer. Appropriate factors causing this phenomena have not yet been elucidated, but the fact that interaction between arrayed amino groups is stronger than that for carboxyl groups seems to be one of reasons. The magnitude of the interaction has been measured by chemical force microscopy.[51-53] If such the stronger interaction contributed to closely packed monolayer, it would prevent penetration of species in the electrolyte solution. The linear E_p change with slopes around -30 mV / pH was also observed at pH < 6.4. It is likely that the eq. (2) where R = $(CH_2)_n$-NH_3^+ is an appropriate reaction in this pH region.

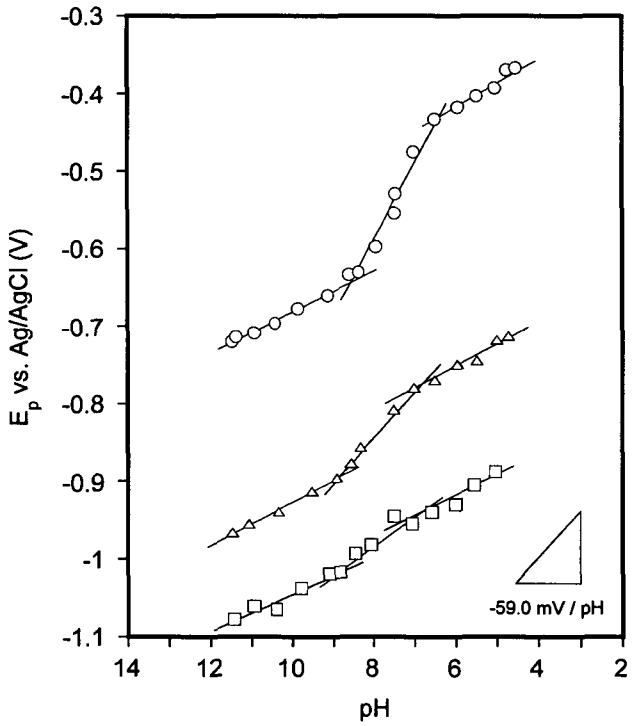

Figure 1-7. Plots of peak potentials of cathodic waves due to reductive desorption of NH_2-terminated alkanethiol SAMs of n = 2 (○), 8(Δ), and 11(□) as a function of pH of electrolyte solution.

It has been already reported that pK_a of amino group in SAM tends to be smaller than the original value. For example, 5.3 (capacitance titration)[49] and 3 - 7 (chemical force microscopy)[51-53] were reported. If pH values of 6.4 - 6.8 where the bending points appeared were assumed to be pK_a values of amino groups of the NH_2-terminated SAMs, the titration profiles

shown in Figure 1-7 could be understood. In the pH region between pK_a of NH_2-terminated thiol and pK_a of its SAM, NH_2 of the adsorbed thiol is protonated when it is desorbed from the electrode. Then, the reaction is formulated as

$$Au\text{-}S\text{-}(CH_2)_n\text{-}NH_2 + e^- + 2H^+ \rightarrow Au + HS\text{-}(CH_2)_n\text{-}NH_3^+ \quad (4)$$

The equation includes two protons because of simultaneous protonation of thiolate and amino groups. This should give dependence of E_p on pH whose magnitude is greater than that observed in other pH regions. In case of SAM of 2-aminoethanethiol, E_p changed at $6.4 < pH < 8.6$ with a slope of -110 mV / pH, which is close to the value expected from the Nernst equation including one electron and two protons. However, such the characteristic profile became dull with an increase in length of the thiols due probably to kinetic factors mentioned above.

1-4. Conclusions

It has been demonstrated in this chapter that reductive desorption of alkanethiol SAMs measured by conventional voltammetry becomes a useful way to evaluate the properties of functional groups substituted the terminals of alkanethiols. The pH dependency of the peak potentials of the reductive desorption wave is a significant clue to elucidate acidity of functional groups in arrayed molecules in SAMs and those dissolved in solution. That also gives some information concerning packing conditions of the monolayer and affinity of the layer surface. The latter information is obtained from degree of deviation of the cathodic wave from the ideal one based on the Nernstian behavior. However, a way to evaluate the degree was not developed in this study. In order to develop such the way, it would be needed to elucidate kinetic factors controlling shape and position of the cathodic wave and successive research works are underway aiming development of a method to clarify the SAM structure by electrochemical means.

Chapter 2

Voltammetric characterization of interfacial properties between alkanethiol self-assembled monolayers and ionic liquid

2-1. Introduction

Salts that are liquid states in room temperature are called ionic liquids, it is possible to use them as liquid electrolytes composed entirely of ions. Since the first discovery of the ambient temperature ionic liquid by Hurley and Wier in 1951[64], many classes of molten salts have been investigated. They have many desirable properties as solvents, including high ionic conductivity, negligible vapor pressure, wide electrochemical windows, thermal stability, and nonflammability. Especially, imidazolium-based ionic liquids are receiving great attentions for use in a variety of commercial applications such as batteries, capacitors, and electroplating. The general physical and chemical properties of them have been well characterized[65-68] since they were first prepared in 1982 by Wilkes et al.[69] However, knowledge of the electrochemical behavior of the ionic liquids is still limited so far.

As described in chapter 1, reductive desorption of an alkanethiol-SAM is a powerful tool to investigate interfacial properties between a monolayer and electrolyte solutions. The peak potential of the reductive desorption depends on not only properties of monolayer but also some ambient parameters including pH of electrolyte solution, electrolyte cations. To extend applicability of the SAM-desorption technique, the reductive desorption of alkanethiols in imidazolium-based ionic liquids was conducted.

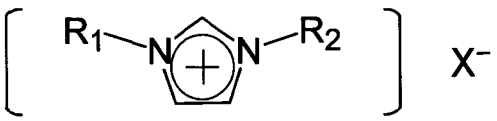

Structure of imidazolium-based ionic liquids.

2-2. Experimental Section

Materials. 1-Ethyl-3-methylimidazolium tetrafluoroborate ($EMIBF_4$) was purchased from Kanto Chemical Co., Inc. 1-Ethyl-3-methylimidazolium bis(trifluoromethylsulfonyl)imide (EMITFSI) was synthesized by metathesis reaction of 1-ethyl-3-methylimidazolium bromide (Aldrich) and lithium bis(trifluoromethylsulfonyl)imide (Aldrich) in water.[66] The resulted EMITFSI separated from the aqueous phase was washed thoroughly with pure water. To ensure complete removal of solvent water, the final products were dried in vacuum at 110 °C for 24h and stored in a dry-argon atmosphere. All other chemicals were of reagent grade and used without further purification. Water used in this study was purified by a Milli-Q Gradient A10 (ρ > 18.2 MΩcm). Au(111) electrodes coated with alkanethiol-SAMs were prepared by the same procedure described in chapter 1.

Methods. Electrochemical measurements were performed by using HSV-100 (Hokuto Denko Co.) in a dry-argon atmosphere glove box. A conventional three electrode cell was employed, with a quasi-reference electrode of Ag wire in $EMIBF_4$ or EMITFSI containing 0.1 mol dm^{-3} $AgBF_4$ or AgTFSI, respectively. In addition, an active area of an Au working electrode was restricted by a Teflon-coated O-ring to be 0.40 ± 0.02 cm^2. The potential of the quasi-reference was then calibrated against the redox potential of ferrocen/ferrocenium ($Fc^{0/+}$) process used as an internal reference.

2-3. Results and Discussion

Figure 2-1 shows linear sweep voltammograms of Au(111) electrodes coated with alkanethiol-SAMs having several different chain lengths. The data were taken at a scan rate 100 mVs^{-1} in EMITFSI. As observed in aqueous solutions (Figure 1-1), cathodic waves associated with reductive desorption of thiol appeared, and the peak potential was negatively shifted with an

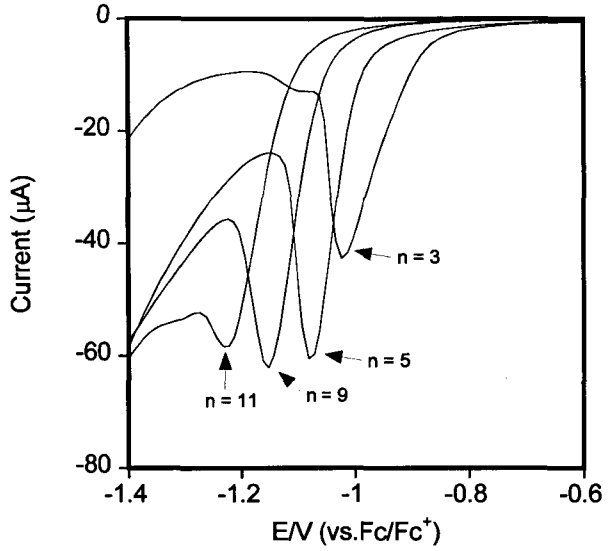

Figure 2-1. Linear sweep voltammograms of alkanethiol-SAMs of various chain lengths (*n*) on Au(111) electrodes taken at 100 mVs^{-1} in EMITFSI.

increase in the chain length of thiol molecule. The charges calculated by integration of cathodic waves of (7.5 ± 0.6) x 10^{-5} C cm^{-2}, agreed well with the value expected for the coverage $\sqrt{3}$ x $\sqrt{3}$ R30° structure of an alkanethiol-SAM on Au(111), suggesting that SAMs kept the packed structure in ionic liquids. Though the charges of desorption peak is usually greater than that expected from the packed $\sqrt{3}$ x $\sqrt{3}$ R30° structure by the contribution of the double layer charging, the obtained value in EMITFSI was good accordant with theoretical one , which might be due to small capacitance of the double layer in EMITFSI determined to be 12 μF / cm^2 on a dropping mercury electrode by Koch and co-worker[70].

The peak potentials (E_p) of reduction waves are plotted as a function of chain length (n) in Figure 2-2. In the same manner as the case of KOH aqueous solution, the negative shift of E_p with elongation of the alkyl chain was observed and was reasonably described by a straight line with a slope of ca. -20 mV / n in both ionic liquids. However, the line was located at more positive by about 50 mV than that obtained in aqueous solution. Since both $EMIBF_4$ and EMITFSI have the same cation of EMI and the corresponding anions, namely they contains no

proton, the desorption of SAMs can be formulated by Au-S-R + e^- → Au + $^-$S-R, which is the same as the equation for the SAM desorption in strong alkaline solution. As mentioned in chapter 1, affinities between electrolyte cations and the terminal groups of SAMs on the electrode influence the desorption behavior of SAM because cations must penetrate through the packed alkyl layer for charge compensation of the generated thiolate anions. Thus, it should be easier for hydrophobic EMI cations to approach and go into the monolayer having methyl terminal groups than protons or potassium cations in aqueous solution, results in positive shift of the desorption potential in ionic liquids.

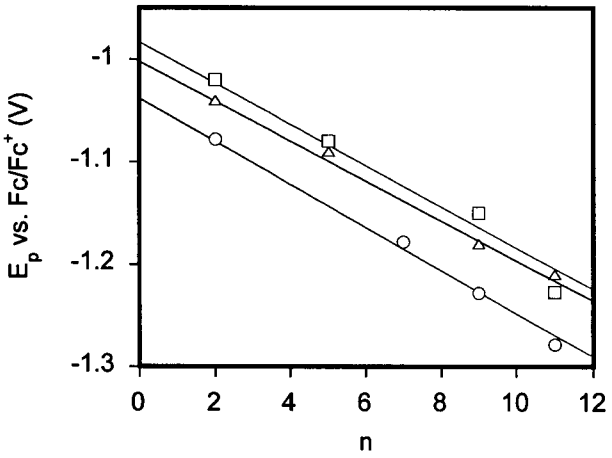

Figure 2-2. The peak potential vs. n for the reductive desorption of CH_3-terminated alkanethiol SAMs measured at 100 mVs^{-1} in 0.5 mol dm^{-3} KOH aqueous solution (○), EMI-BF_4 (Δ), and EMI-TFSI (□)..

However, a small difference in E_p between ionic liquids was observed in spite of the same EMI cation. This implies that there is another parameter influencing the desorption behavior of the monolayers. To reveal this, desorption studies were conducted by Au(111) electrodes coated with SAMs having different terminal groups of -CH_3, -COOH, and -SO_3Na. Figure 2-3 shows linear sweep voltammograms taken at 100 mVs^{-1} in KOH aqueous solution, EMIBF_4, and EMITFSI, respectively. In aqueous solution, SAM having more hydrophilic terminal groups desorbed at more positive potentials, whereas the opposite order was observed in EMIBF_4,

suggesting strongly the presence of affinities between EMI cations and terminal groups of SAMs. It is, however, noteworthy that this behavior was more conspicuous in EMITFSI. As comparing those ionic liquids, it is considered that anions should act as another factor on desorption behavior. In aqueous solution, ions are solvated by water molecules, but ionic liquids dose not have such solvent molecules. However, the presence of the ionic association or the ionic components that cannot contribute to ionic conduction in the ionic liquids has been reported.[71] If those ionic associations contributed to the reductive desorption of SAMs on the electrodes, not only cations but also anions should influence desorption behavior. Thus, the significant

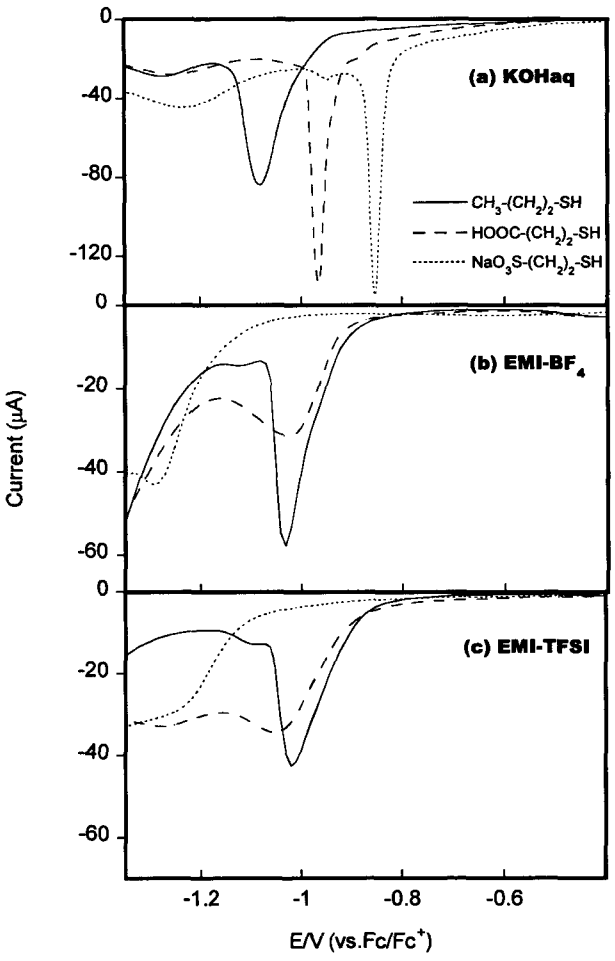

Figure 2-3. Linear sweep voltammograms of CH_3-$(CH_2)_2$-SH, HOOC-$(CH_2)_2$-SH, and NaO_3S-$(CH_2)_2$-SH coated Au(111) electrodes, taken at 100 mVs^{-1} in 0.5 mol dm^{-3} KOH aqueous solution (a), EMI-BF_4 (b), and EMI-TFSI (c).

difference of desorption waves observed in EMITFSI compared to those in aqueous solution, would be due to strongly hydrophobic TFSI anions.

2-4 Conclusions

In this chapter, reductive desorption of alkanethiol-SAMs on Au(111) in ionic liquids was investigated. The peak potentials of the reductive desorption wave gives significant information concerning affinities between cations and functional groups substituted the terminals of alkanethiols. Furthermore in the cases of ionic liquids having the same cation, the different desorption potential, which induced by difference in properties of anion, could be observed. Such a behavior suggests that cations are associated by anions in ionic liquids just like salvation by water molecules in aqueous solutions, and has been first detected dynamically in this study. The desorption method is demonstrated to be a useful method to evaluate electrochemical behavior of ions in ionic liquids.

Chapter 3

Development of Electrochemical Methods to Elucidate Dynamic Parameters of Lipid Molecules in Bilayer Membrane

3-1. Introduction

The bio-membrane, which plays important roles such as metabolism, material transport, information transfer, and segregation and fusion of cells, is composed of the lipid bilayer and protein bio-molecules fixed in it. This membrane is not a mere separator but molecular assembly exhibiting dynamic relocation. Activity of the membrane itself and combination of the membrane movement and functions of the fixed bio-molecules provide the ingenious reaction of a living body. Therefore, the bilayer has been extensively studied to elucidate mysterious functions of the bio-cells.

For such studies, two types of the lipid bilayers are mainly used; one is a liposome that is a vesicle of lipid membrane[72-81] and the other is a plane lipid membrane formed in a small pore.[82-85] The latter is useful for studying material transfer across the membrane by electrochemical means. However, stability of the membrane is not sufficient for measurements that need relatively long time. The liposome is preferred in the measurements for getting information concerning such the movement as flow and flip-flop. The spectroscopy measurements including fluorescent probe methods are ordinary ways,[86,87] and they need relatively long measurement time and large amount of lipid molecules because of sensitivity. Therefore, solution, in which liposomes including fluorescent molecules are dispersed, is used and the average values for all liposomes in the solution are obtained as measurement results.

Recently, the supported bilayer lipid membrane is attracting great attention as another type of membrane that is applicable to several kinds of electric and electrochemical devices.[85,88-93] One of such bilayer membranes, the bilayer composed of lipid monolayer and SAM of

alkanethiol on a metal substrate, which is schematically illustrated in Figure 3-1, is reported as a new artificial bilayer membrane.[94-97] Since this membrane is very stable, attempts have been made to fabricate intelligent biosensors.[96,97] To elucidate static properties of the bilayer, some electrochemical measurements of electrodes coated with the bilayer membranes have been conducted.[94] In this chapter, it is described that this bilayer membrane is also useful for studies on dynamic relocation of lipid molecules in the bilayer membrane, and the principle of novel electrochemical methods to evaluate fluidity of lipid membrane and formation rate of the bilayer membrane by fusion of the liposome is concisely introduced.

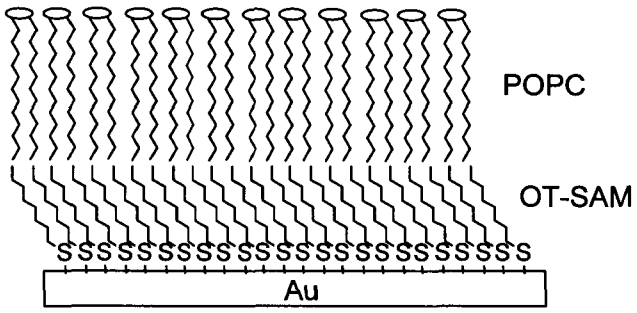

Figure 3-1. Schematic illustration of a bilayer membrane composed of self-assembled monolayer of alkanethiol (Thiol-SAM) on Au substrate and lipid molecules. Inclination of thiol molecules in SAM is considered.

3-2. Experimental Section

Materials. Ethanol and 2-propanol used as solvent were purified by distillation. Water used for preparation of aqueous solutions was purified by a Milli-Q system (Millipore). All other chemicals of analytical grade including 1-palmitoyl-2-oleoylphosphatidylcholine (POPC), cholesterol, and alkanethiols were used without specific purification. The alkanethiols used in this study were octanethiol (OT), dodecanethiol (DDT), and hexadecanethiol (HDT). An Au(111) electrode substrate was prepared by vacuum evaporation of Au, as described in chapter 1. The

Au(111) electrode coated with a alkanethiol-SAM was prepared by immersing the Au electrode in an ethanol solution containing 1 mmol dm^{-3} alkanethiol. The resulting electrode will be denoted here as OT|Au, DDT|Au, and HDT|Au, respectively.

POPC liposome-dispersed solution was prepared as follows. 10 mmol dm^{-3} POPC dissolved in $CHCl_3$ was put in a round bottom flask, and then the solvent was evaporated under reduced pressure using a rotary evaporator to deposit POPC thin films, which were then dried in vacuum for 1 day. The resulting POPC films were dissolved in 2-propanol to give 40 mmol dm^{-3} POPC, and 0.05 cm^3 of this solution was added to 1 cm^3 of 20 mmol dm^{-3} Tris-HCl buffer containing 0.15 mol dm^{-3} NaCl (pH 7.3), followed by agitating vigorously for 10 min to give a suspension of POPC liposomes. When POPC liposomes containing 20 mol% cholesterol were prepared, $CHCl_3$ containing 2.0 mmol dm^{-3} cholesterol and 8.0 mmol dm^{-3} POPC was used as a starting solution. The Au(111) electrode coated with the bilayer of OT and POPC was prepared by immersing the OT|Au electrode in the prepared liposome-dispersed solution for 3 h. The electrode coated with OT and pure POPC and that coated with OT and mixed layer of POPC and cholesterol will be denoted as POPC|OT|Au and POPC-Chl|OT|Au, respectively.

Methods. Electrochemical experiments were carried out using a glass tube cell described in chapter 1. After pouring the electrolyte solution, the cell was capped with a silicon rubber equipped with an Ag|AgCl|KCl(sat.) reference electrode and a Pt foil counter electrode. Measurements including AC impedance were made using an ALS electrochemical analyzer (Model 602A).

3-3. Results and Discussion

3-3-1. Electrochemical desorption of bilayer

Desorption of the alkanethiol-SAM from metal electrode is possible by electrochemical reduction. Several studies including those described in chapter 1 and 2 have revealed that the peak potential of the reductive desorption of alkanethiol depends on several parameters including pH of electrolyte solution, kind of electrode metal,[40,56,98] length of alkyl group[40] and kind of terminal substituent of the alkyl group.[59,99]

Figure 3-2A shows linear sweep voltammograms of Au electrodes coated with OT-SAM, DDT-SAM, and HDT-SAM. The OT|Au gave a reduction wave with a current peak at -0.95 V. Integration of the wave gave 30.5 μC, from which amount of OT was estimated to be 7.9 x 10^{-10} mol cm^{-2}. This value was close to the value expected for the alkanethiol SAM with ($\sqrt{3}$ x $\sqrt{3}$)R30° configuration, suggesting that fully packed monolayer was obtained. In case of alkanethiol-SAM having relatively short alkyl group like OT-SAM, the quantitative evaluation

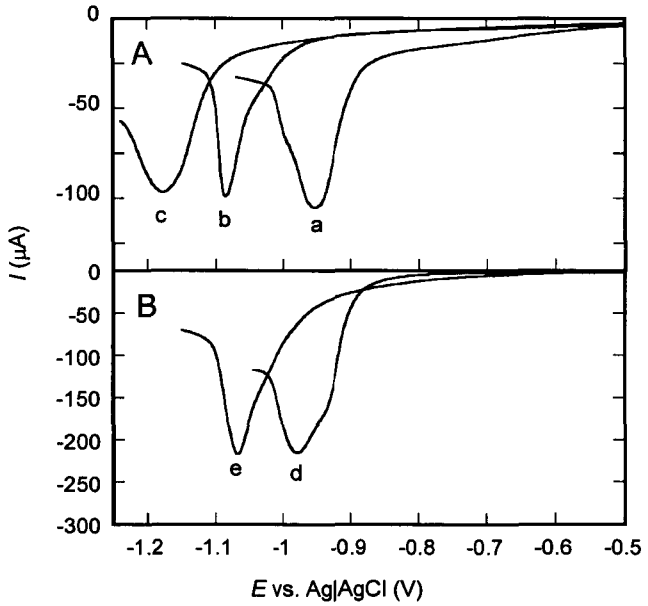

Figure 3-2. Linear sweep voltammograms of OT|Au (a), DDT|Au (b), HDT|Au (c), POPC-Chl|OT|Au (d), and POPC|OT|Au (e) electrodes taken at 0.1 V s^{-1} in 1 mol dm^{-3} KCl solution.

utilizing charges consumed by desorption is reliable. However, as alkyl group is longer, change in capacitance of the electric double layer caused by the electrochemical desorption of SAM becomes larger. Then, charges due to the capacitance changes cannot be ignored, giving large errors in the quantitative determination of thiol molecules by the desorption experiments.[100] As recognized from Figure 3-2A, an increase in the length of the alkyl group in thiol molecule made potential for induced reductive desorption shift negatively. This potential shift is due to the intermolecular forces between alkyl groups of alkanethiol molecules.

The electrochemically reductive desorption was also attempted for the POPC|OT|Au and the POPC-Chl|OT|Au, and the obtained voltammograms are shown in Figure 3-2B where distinct reduction waves are seen for both the electrodes. Comparisons of peak potential observed for the POPC|OT|Au with that for the OT|Au revealed that presence of POPC layer on OT-SAM caused negative shift of a reduction wave due to OT desorption. It is then quite natural to suppose that POPC-coating exhibits similar effects to the case of an increase in alkyl group. A POPC molecule has two alkyl chains, of which length are C_{16} and C_{18}. If POPC and OT-SAM gave the perfectly rigid bilayer membrane, blocking effect due to membrane thickness would be larger than that of C_{24}. However, the obtained results were contrary to such an anticipation because the peak potential obtained for desorption of the POPC|OT|Au was much positive than that obtained for the DDT|Au having length of C_{12}. As well known, lipid molecules in the bilayer possess fluidity.[73-78] It can be, therefore, understood that the effect of negative shift of the reduction potential is smaller than the expected one if fluidity of the POPC layer on OT-SAM is considered.

Another thing that is noteworthy in Figure 3-2B is magnitude of the reduction wave. The voltammogram of POPC|OT|Au gave a current peak of ca. 230 μA, which is more than twice that for OT|Au. This clearly indicated that the reduction wave of POPC|OT|Au included charges due to changes in capacitance of the electric double layer as already mentioned, and then this should be one of facts evidencing the bilayer membranes were definitely formed on the POPC|OT|Au electrode. Also such the large changes in the capacitance were useful for

monitoring formation of the bilayer by capacitance measurements, as will be shown in the next section.

The voltammogram (d) obtained for the POPC-Chl|OT|Au electrode indicates a reduction wave at -0.98 V that was apparently positive than the wave observed for the POPC|OT|Au though that potential was a little positive than that for the OT|Au. In the case of lipid bilayer membrane, it is well known that addition of cholesterol gives two opposite effects that are enhancement of fluidity and hardening of membrane.[101-104] The several conditions such as kind of lipid, amount of cholesterol, and temperature are related to the actual effect. Since positive shifts of the desorption wave should represent increase in fluidity of the membrane as described above, the results shown in Figure 3-2B allowed us to suppose that addition of cholesterol in the bilayer under the present condition enhances fluidity of the membrane.

3-3-2. Impedance measurements of bilayer for evaluating rates of bilayer formation

As well known, when an electrode is polarized in electrolyte solution, the electric double layer is developed at the electrode surface. The presence of alkanethiol-SAM or bilayer of lipid and alkanethiol-SAM on the electrode surface causes enlargement of distance between surface of a metal electrode substrate and the outer Helmholtz plane where potential changes appear. Consequently, electrochemical capacitance decreases.

Figure 3-3 shows the Nyqust plots obtained by the impedance measurements of the OT|Au and the POPC|OT|Au electrodes. The measurements were conducted by imposing the ac signal of 10 mV (peak to peak) to the electrode potential at 0 V vs. Ag|AgCl. The frequencies chosen were from 1 kHz to 100 Hz. Both electrodes showed a decrease in impedance along the imaginary axis (Z_{im}), allowing that a series circuit of a resistor and a capacitor is regarded as an appropriate equivalent circuit for those electrodes. The capacitance obtained for the former and the latter electrodes was 1.25 μF and 0.65 μF, respectively. The difference in the capacitance reflected definitely the difference in thickness between monolayer and bilayer. In this case, capacitance can be evaluated by measurement with a fixed frequency. Then, changes in

capacitance were measured to monitor formation of the bilayer. The capacitance of the OT|Au electrode was measured by applying AC signal with 810 Hz in phosphate buffer solution. While the capacitance measurement was continued, POPC liposome-dispersed solution was added to the solution by using a syringe. Then, capacitance changes in the course of time were monitored. The same experiments were made by changing POPC concentration in the solution, and the

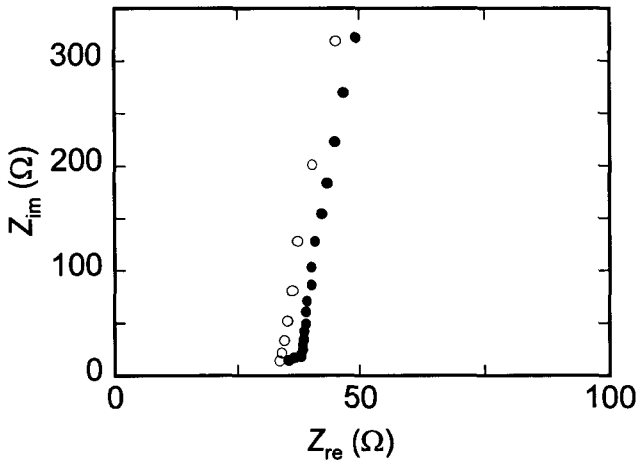

Figure 3-3. Impedance plots of OT|Au (●) and POPC|OT|Au (○) electrodes taken 0 V vs. Ag|AgCl in 1 mol dm^{-3} KCl solution.

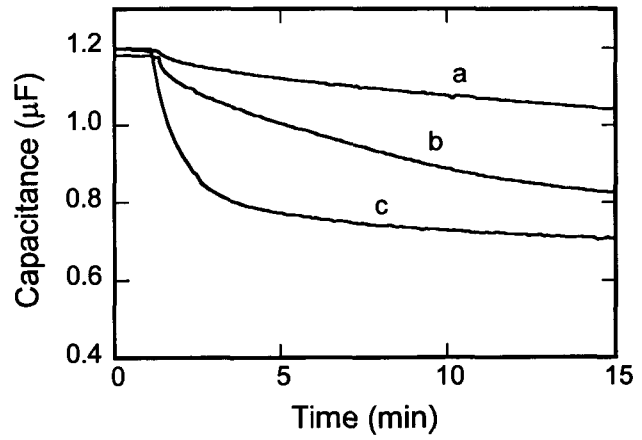

Figure 3-4. Changes in capacitance of the OT|Au electrode in 1 mol dm^{-3} KCl solution caused by addition of POPC in concentrations of 4 (a), 10 (b), 40 (c) μmol dm^{-3}.

obtained results are shown in Figure 3-4. The capacitance decreased with time for all cases but their rate became large with an increase in POPC concentration.

Since the bilayer of OT and POPC is formed by fusion of POPC liposome to OT-SAM, the bilayer parts should generate at places where liposomes attach to the surface of OT-SAM. Then, the areas of the bilayer parts increase with time, causing a decrease in capacitance of the electrode. If capacitance of bilayer parts and that of OT-SAM parts are denoted as C_b and C_m, respectively, the whole capacity of the electrode (C_{all}) is equal to $C_b + C_m$. Since alkyl chains occupy most of both POPC and OT molecules, the bilayer and OT-SAM have different thickness but their dielectric constants (ε) can be regarded as the same. Therefore, C_{all}, C_b, and C_m are formulated as

$$C_{all} = C_b + C_m = \varepsilon (S_b/\delta_b + S_m/\delta_m) \qquad (1)$$

where S_b and S_m are areas of bilayer parts and OT-SAM parts, respectively, and δ_b and δ_m are their thickness.

If capacitance of the POPC|OT|Au and the OT|Au electrodes is denoted here as C_B and C_M, respectively, they are formulated as

$$C_B = \varepsilon (S_{all}/\delta_b) \qquad (2)$$

$$C_M = \varepsilon (S_{all}/\delta_m) \qquad (3)$$

where S_{all} is area of the electrode. Since $S_{all} = S_b + S_m$, eq. (1) can be changed into eq. (4).

$$\begin{aligned} C_{all} &= \varepsilon S_{all}\{\theta/\delta_b + (1 - \theta)/\delta_m\} \\ &= \theta C_B + (1 - \theta) C_M \end{aligned} \qquad (4)$$

where θ (= S_b/S_{all}) is a ratio of areas occupied by the bilayer on the electrode. Accordingly, the changes in capacitance shown in Figure 3-4 can be converted to changes in θ by using eq. (4).

I attempted to analyze the results shown in Figure 3-4 from a viewpoint of adsorption of POPC molecules on the OT-SAM surface. It has been then found that the bilayer formation proceeds with the first-order. The adsorption rate with the first-order is given by

$$\ln(1 - \theta) = -kct \qquad (5)$$

where k and c are rate constant and concentration, respectively. From eq. (4), $(1 - \theta)$ is given by

$$1 - \theta = (C_{all} - C_B)/(C_M - C_B) \quad (6)$$

Plots of the $\ln(1 - \theta)$ values obtained from the results shown in Figure 3-4 as a function of time gave linear relations shown in Figure 3-5. Similar experiments were made for other POPC concentration ranging 10-180 μmol dm^{-3}, and slopes of the relation between $\ln(1 - \theta)$ and time were estimated. Then the k values were obtained from the ratio of the slopes to POPC

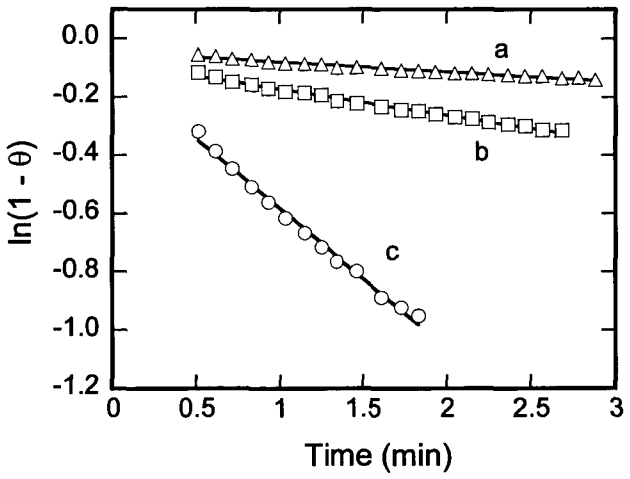

Figure 3-5. Replots of the capacitance changes shown in Fig. 4 based on eq. (5) and (6) in text.

concentration. Figure 3-6 shows plots of the k values as a function of the POPC concentration. Almost the same value was obtained for the formation of POPC|OT bilayer. This indicates that eq. (5) is adequate and that fusion of POPC liposome to OT-SAM is not rate-determining step in this case. Since the POPC concentration range chosen in this study was very dilute, the formation rate might be controlled by diffusion of POPC liposomes in the solution. In other words, it is expected that the formation rate does not obey the first-order in higher concentration. If so, information of rate of fusion between liposomes and OT-SAM would be obtained.

In Figure 3-6, results obtained for the POPC-Chl|OT-SAM are also given. For these cases total concentration of POPC and cholesterol was chosen as the concentration shown in this figure. Apparently, the k value obtained was smaller than that obtained for the POPC|OT-SAM. As already mentioned above, the presence of cholesterol influences fluidity of POPC layer. However, it was not expected that the fluidity concerned the formation rate because the formation rate of the bilayer is controlled by diffusion of POPC as shown above. Although the factors causing the strange results could not be elucidated in this study, the most plausible reason might be differences in concentration of liposomes. The liposome can take several forms such as a multilamelar vesicle and an unilamellar vesicle. The forms are influenced by preparation method,

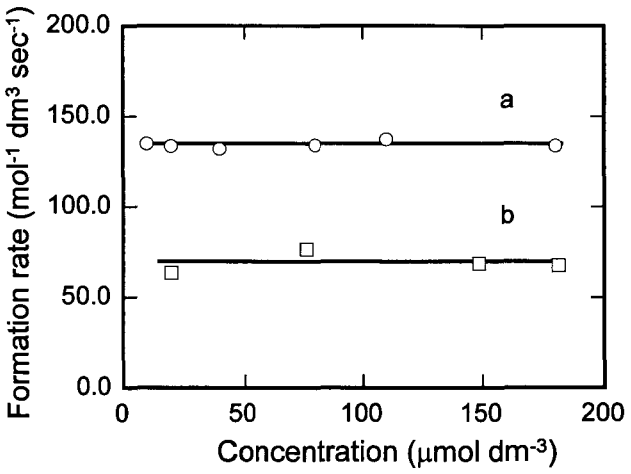

Figure 3-6. Plots of formation rates for bilayer of PCOP|OT-SAM (a) and PCOP-Chl|OT-SAM (b) as a function of total concentration of PCOP and cholesterol added to the solution.

kind of lipid, preparation conditions, and so on. Even if the lipid concentration is the same, the concentration of liposome that is number of liposomes in solution must be changed by changes in form and/or size. If the presence of cholesterol was one of the parameter causing a decrease in the liposome concentration, the results shown in Figure 3-6 can be understood.

3-4. Conclusions

Electrochemical methods to evaluate dynamic parameters of lipid membrane have been developed in this chapter. Since there is no other method allowing kinetic studies on a planar bilayer membrane, the electrochemical methods introduced here have high potential allowing to elucidate kinetic parameters that have never been obtained. In particular, I would like to emphasize a point that absolute values of the formation rate can be obtained from the capacitance measurements, as shown in Figure 3-5. In the case of measurements of liposomes involving fluorescence probes, the obtained rate constant should be different from the real one as judged from the measurement principle. Simplicity of the measurement instruments including the electrochemical cell is another merit and it allows combination of these measurements with another measurements.

Chapter 4

Spatial distribution of domains in binary self-assembled monolayers of thiols having different lengths

4-1. Introduction

Chemical modification by monolayers of ω-substituted alkanethiols is widely used for creating surfaces with desired properties, and further adjustment of their properties can be conducted by coadsorption of two or more kinds of thiols.

If one would like to prepare a desired surface by coating with a SAM composed of different thiols, it is necessary to check how the thiols are distributed on the surface, but this is not easy to determine. However, recent improvements of scanning tunneling microscopy (STM) have made it possible to observe distinct thiol molecules constituting a SAM with tunneling currents of the order of picoamps.[38,39] The spatial distribution of thiols in binary SAMs was also revealed, and so far, two modes have been confirmed: randomly mixed structures for thiols having comparable lengths[39,105], and phase-separated structures for thiols of different lengths.[59,105-107] In the latter case, longer thiols tend to make separated domains, around which shorter thiols form a continuous SAM. Those results suggest that the degree of difference in the lengths of thiols composing the binary SAMs influences the spatial distribution of the thiols. This chapter focuses on such relationship. 3-Mercaptopropionic acid (MPA) was used as a short thiol and one of 1-hexadecanethiol (HDT), 1-dodecanethiol (DDT), 1-decanethiol (DT), and 1-octanethiol (OT) was used as a long thiol. The binary SAMs of MPA and a long thiol were prepared by the coadsorption technique, and electrochemical desorption experiments and STM observations of the prepared binary SAMs were carried out. The discussion focuses briefly on the degree of difference in the intermolecular affinities inducing the packing SAM between MPA and the long thiol.

4-2. Experimental Section

Materials. OT, DT, DDT, and HDT purchased from Wako pure chemicals and MPA purchased from Dojindo Laboratories were reagent grade chemicals and were used as received. Water used for preparation of electrolyte solutions was purified by a Milli-Q Gradient A10. All other chemicals were of reagent grade and used without further purification. An electrode substrate used in this study was an Au-coated mica sheet having atomically flat (111) terraces. This electrode was prepared by the same method described in chapter 1.

Simultaneous adsorption of two thiols having different lengths for the formation of their binary SAMs was performed by immersing the Au substrate for 1 h in an ethanol solution containing these thiols. As mentioned above, MPA was used as the short thiol for all cases and its concentration was fixed to 1 mmol dm^{-3}, whereas the concentration of the long thiol was varied from 0.1 to 0.3 mmol dm^{-3} to obtain the binary SAMs of different composition. The prepared electrode was then rinsed with water and dried in N_2 atmosphere. The electrodes coated with thiol SAMs were denoted here by the abbreviations of the components of the coated SAMs, e.g. MPA|Au and OT-MPA|Au.

Methods. Electrochemical experiments were carried out using a glass tube cell described in chapter 1. After pouring electrolyte solution, the cell was capped with a silicon rubber equipped with a reference electrode of Ag|AgCl in KCl-saturated aqueous solution and a Pt foil counter electrode. Measurements were made by using an ALS-701 electrochemical analyzer. The electrolyte solution used for electrochemical desorption of thiols was 0.5 mol dm^{-3} KOH aqueous solution and it was deaerated by bubbling N_2 gas for 15 min at least prior to the desorption experiments. The selective desorption of MPA in the binary SAMs was made by polarizing the electrode at a given potential.

STM observations of the prepared electrodes were carried out in air by using Nanoscope III STM apparatus equipped with a 'Pico Amp' low current pre-amplifier and a 'Tip-View' STM head (Digital Instruments). The electrochemically pretreated specimen was rinsed with water

followed by blowing dry N_2 gas on its surface for 5 min at least to obtain completely dry condition. All images were taken in the constant-current mode with a tunneling current between 2 and 30 pA and a bias voltage between 700 and 1500 mV. The STM tip used was a Pt-Ir wire sharpened electrochemically in aqueous solution containing 6 mol dm^{-3} NaCN and 2 mol dm^{-3} KOH by applying 12 V AC.

4-3. Results and Discussion

4-3-1. Coadsorption of MPA and the long thiol

Figure 4-1 shows linear sweep voltammograms of the OT-MPA|Au electrodes taken in 0.5 mol dm^{-3} KOH. The ethanol immersion baths used for preparation of the electrodes giving voltammograms a, b, and c contained 1 mmol dm^{-3} MPA and 0.1, 0.2, and 0.3 mmol dm^{-3} OT, respectively. The remarkable reduction peak appeared in the voltammogram a is assignable to desorption of MPA, because a single component MPA monolayer showed a desorption peak at –0.79 V. When the OT concentration in the immersion bath was increased, the MPA desorption peak decreased, while another reduction peak observed at around –0.9 V became larger. The latter reduction peak should represent the reductive desorption of OT although the OT|Au electrode gave a desorption peak at –0.99 V in its voltammogram taken under the same conditions. Simultaneously, negative shifts of the MPA desorption peak was accompanied with a decrease in the peak height. The potential shifts of the reductive desorption peaks of thiols in binary SAMs as compared with the original potential of each single component SAM were found for the first time by Kakiuchi's group.[59,99] It is presently believed that such potential shifts are reflected by partial dissolution of thiol molecules to domains of the other thiol in the binary SAMs. Therefore, in the case of the binary SAMs of OT-MPA, two thiols form individual domains, as will be shown later, but some amount of them might be slightly dissolved into each other at the boundaries between OT and MPA domains.

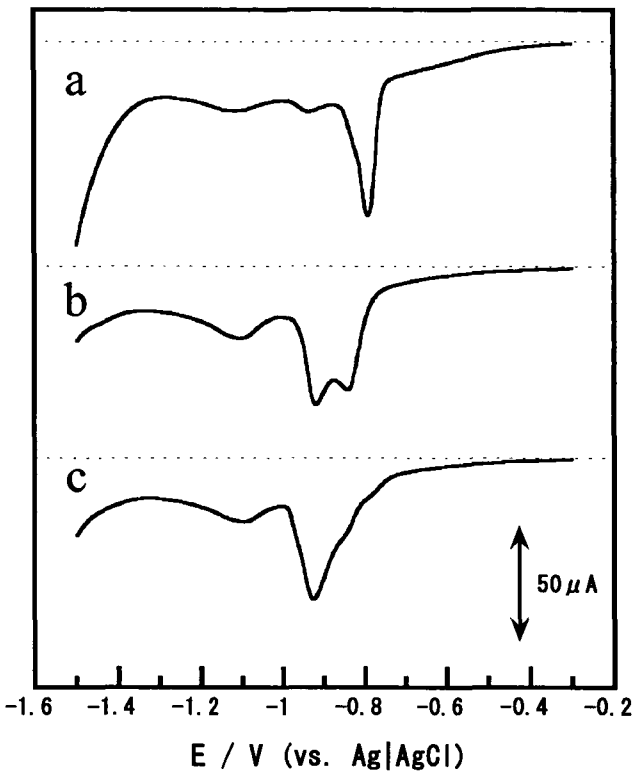

Figure 4-1. Linear sweep voltammograms taken in 0.5 mol dm^{-3} KOH at 0.1 V s^{-1} of OT-MPA|Au electrodes prepared from an ethanol solution containing 1 mmol dm^{-3} MPA and (a) 0.1, (b) 0.2, and (c) 0.3 mmol dm^{-3} OT.

The reductive desorption behavior of the binary SAMs of DT-MPA, DDT-MPA, and H DT-MPA was also investigated by linear sweep voltammetry and the results obtained are shown in Figure 4-2. The immersion baths used for these binary SAMs contained 1 mmol dm^{-3} MPA and one of the long thiols in 0.2 mmol dm^{-3}. All voltammograms show two resolved reduction peaks indicating coadsorption of two thiols on the Au substrates. It is recognized by comparing voltammograms shown in Figure 4-1b and Figure 4-2 that the reduction peak due to desorption of the long thiol shifts negatively with an increase in chain length of the long thiol. This behavior is well reflected by the relationship between the chain lengths of alkanethiols and the reductive desorption potentials of their SAMs, which was elucidated by Porter et al. for single component SAMs.[40] The total amounts of the adsorbed two thiols on each electrode evaluated by

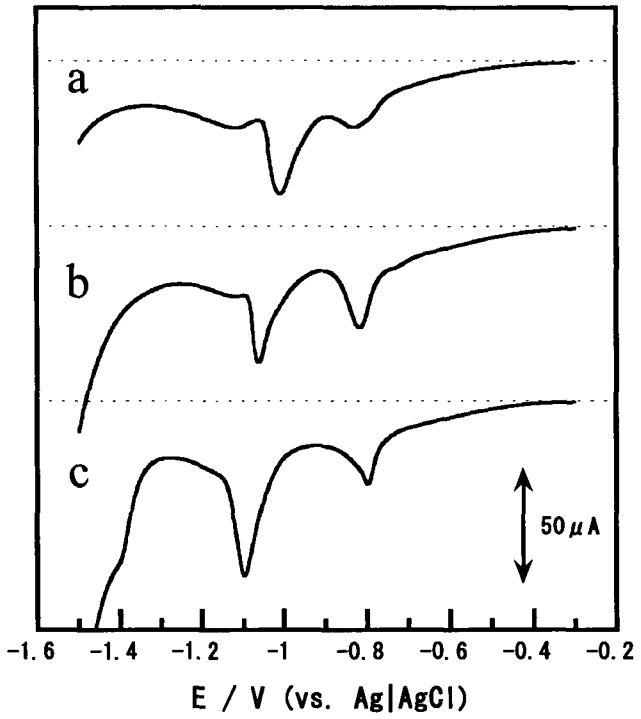

Figure 4-2. Linear sweep voltammograms taken in 0.5 mol dm^{-3} KOH at 0.1 V s^{-1} of (a) DT-MPA|Au, (b) DDT-MPA|Au, and (c) HDT-MPA|Au electrodes. The electrodes were prepared from the immersion baths containing 1 mmol dm^{-3} MPA and 0.2 mmol dm^{-3} long thiol.

electrochemical means were 7.5 x 10^{-10}, 8.6 x 10^{-10}, 8.0 x 10^{-10}, and 8.8 x 10^{-10} mol cm^{-2} for the binary SAMs of OT-MPA, DT-MPA, DDT-MPA, and HDT-MPA, respectively. All values were roughly accordance with the value expected for the alkanethiol SAM with ($\sqrt{3}$ x $\sqrt{3}$)R30° structure (7.6 x 10^{-10} mol cm^{-2}), implying that fully packed monolayers were obtained for all cases. In the cases that a little larger amount of thiols than the theoretical value was obtained, the reduction wave might include electricity used for charging the double layer whose capacity should be increased upon desorption of the thiol SAM.[57]

4-3-2. Selective desorption of MPA from the binary SAMs

The voltammograms as shown in Figures 4-1 and 4-2 gave information about potentials where desorption of the thiols takes place. However, since a peak potential obtained by scanning electrode potential represents a kinetically determined value, it might be different from the thermodynamic value. As a matter of fact, it has been reported that if the reductive desorption of thiol was induced by polarizing the electrode at constant potential, desorption occurs at more positive potential than the peak potential of the reduction wave observed in the voltammogram.[99] To confirm this thing for the reductive desorption of MPA, the reductive desorption experiments were made at various potential scan rates. The voltammograms obtained are shown in Figure 4-3a, and plots of their peak potentials as a function of the potential scan rate gave the results shown in Figure 4-3b. As expected, a decrease in the potential scan rate induced positive shift of the peak potential. In particular, the shifting rate became marked when the potential scan rate was smaller than 20 mV s^{-1}. With this phenomenon in mind, attempt was made to induce the selective desorption of MPA in the binary SAMs by polarizing the electrodes at a constant potential.

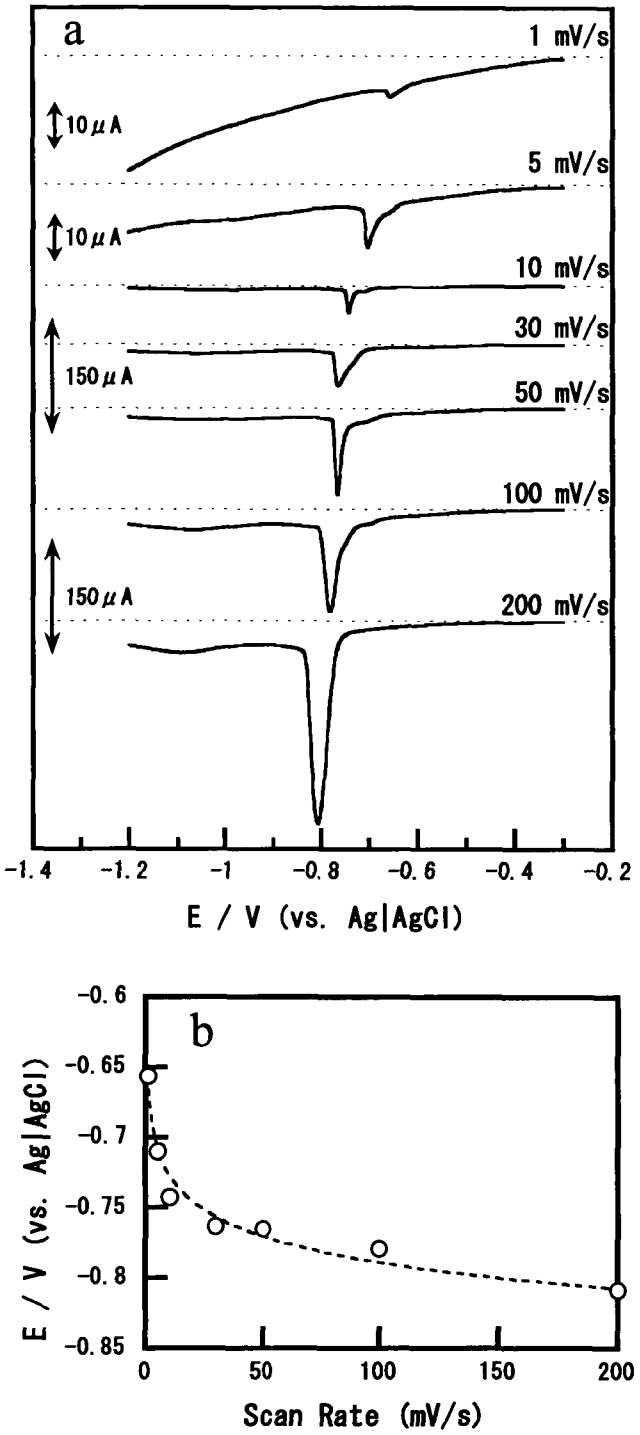

Figure 4-3. (a) Linear sweep voltammograms taken in 0.5 mol dm^{-3} KOH at various potential scan rate of MPA|Au electrodes and (b) plots of their peak potentials as a function of potential scan rate. The electrodes were prepared from the immersion baths containing 1 mmol dm^{-3} MPA.

Figure 4-4 shows linear sweep voltammograms of the OT-MPA|Au electrodes taken in 0.5 mol dm^{-3} KOH. The electrode was prepared using the preparation bath containing 1 mmol dm^{-3} MPA and 0.2 mmol dm^{-3} OT. The voltammogram a is the same as that of Figure 4-1b, whereas the voltammogram b in Figure 4-4 was obtained after polarizing the electrode in the same electrolyte solution at –0.60 V for 10 min. Apparently, the reduction wave due to the MPA desorption disappeared completely in the voltammogram if the electrode was subjected to the polarization prior to the measurement. It is also noted that the reductive desorption wave of OT was negatively shifted by subjecting to the previous polarization and the resulting peak potential of –0.99 V was coincident with that obtained for the single component OT. Those results indicated clearly that the polarization potential of –0.60 V was negative enough to induce the reductive desorption of MPA but not sufficient for the OT desorption. The selective desorption of MPA induced by applying the constant potential of –0.60 V was also possible for the binary SAMs of DT-MPA, DDT-MPA, and HDT-MPA.

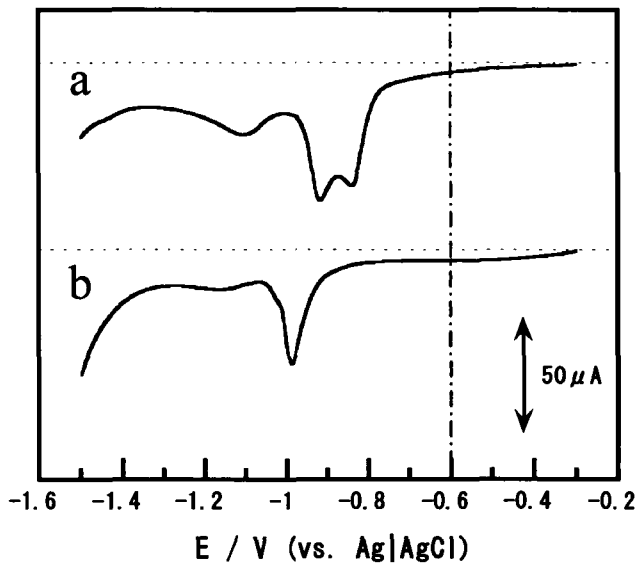

Figure 4-4. Linear sweep voltammograms of OT-MPA|Au electrodes taken in 0.5 mol dm^{-3} KOH (a) before and (b) after polarization of the electrode at –0.60 V vs. Ag|AgCl for 10 min in the same electrolyte solution. The electrodes were prepared from the immersion baths containing 1 mmol dm^{-3} MPA and 0.2 mmol dm^{-3} OT.

After the desorption of MPA from the binary SAMs, the reductive desorption wave of the long thiols alone appeared distinctly, allowing precise estimation of the amount of the long thiols in the binary SAMs. The binary SAMs of OT-MPA, DT-MPA, DDT-MPA, and HDT-MPA were prepared by immersing the Au substrates in the baths containing 1 mmol dm^{-3} MPA and one of the long thiols in 0.1, 0.2, and 0.3 mmol dm^{-3}. Then, total amount of both thiols and the amount of the long thiol were evaluated by the same ways as mentioned above. Plots of the mole fractions of the long thiols in the binary SAMs as a function of the long thiol concentration in the immersion baths are shown by open symbols in Figure 4-5. An increase in the amount of the long thiols in the binary SAMs with increasing the long thiol concentration in the bath was recognized for all cases. The results obtained for the HDT-MPA was well accordance with the reported ones.[57] If the mole fractions were compared at the long thiol concentration of 0.1 mmol dm^{-3}, the value increased in order of OT-MPA < DT-MPA < DDT-MPA < HDT-MPA, indicating that longer thiols tended to occupy higher coverage. It is well known that in the case of

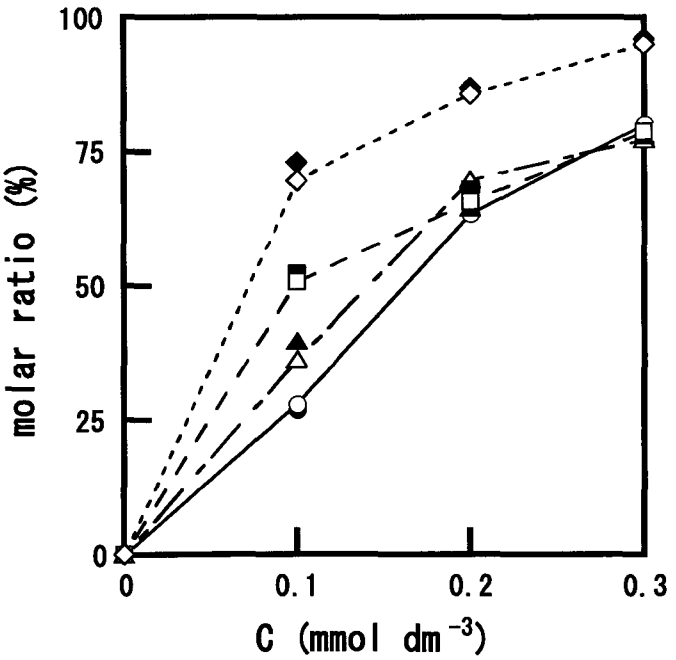

Figure 4-5. Dependence of mole fraction of OT(○), DT(△), DDT(□), and HDT(◇) in their binary SAMs with MPA on the long thiol concentration in the immersion bath. The concentration of MPA was fixed to 1 mmol dm^{-3} for all cases. The solid symbols of ●, ▲, ■, ◆ indicate the values obtained from the STM images of the electrode surfaces.

competitive adsorption of long and short alkanethiols, the long thiol SAM was dominantly formed because exchange of the adsorbed short thiols for the long thiols occurs more easily than the reverse exchange. Whitesides et al. explained thermodynamically such behavior in viewpoint of interactions between adjacent thiol molecules in a SAM, which becomes large when the chain length of thiol is longer.[33] The results shown in Figure 4-5 seem to be reflected well by the theoretical prediction so long as the results obtained for the binary SAMs prepared from the solution containing the long thiol in 0.1 mmol dm^{-3}. However, when the concentration increased, the coverage of OT, DT, and DDT was unified and the value was a little smaller than that of HDT. The results obtained suggested that there is a peculiar difference in the molecular interactions between HDT and other alkanethiols although it was not elucidated in this study.

4-3-3. STM observations of the binary SAMs

The surfaces of the as-prepared OT-MPA|Au, DT-MPA|Au, DDT-MPA|Au, and HDT-MPA|Au were observed by STM to know the spatial distribution of the short and long thiols in their binary SAMs. The areas occupied by MPA and the long thiols could be distinguished for the binary SAMs containing DT, DDT, and HDT by the image contrast indicating differences in height of the surfaces. However, in the case of the OT-MPA binary SAMs, the difference in their lengths was not large enough to make sufficient contrast in the STM image between the areas where OT and MPA were adsorbed. To solve this problem, it was attempted to use the electrode which was previously subjected to the selective MPA desorption as a specimen for the STM experiments. The resulting electrode gave an image showing definitely the distribution of the adsorbed OT molecules. In this case, there arose a doubt whether the distribution of the adsorbed OT varied during the course of the polarization for inducing the selective desorption of MPA. It could be, however, confirmed that the influence of the polarization for 10 min was negligible if any because the images of other binary SAMs taken before and after desorption of MPA gave essentially the same distribution of the long thiols. In other words, the variation in the spatial distribution of the long thiols caused by difference in

chain lengths of the long thiol, as will be shown, were distinctly recognized for both electrodes before and after subjecting to the selective desorption of MPA.

Figure 4-6 shows STM images of 80 nm-square surfaces of the OT-MPA|Au electrodes taken after subjecting the MPA desorption. The electrodes were prepared from the immersion baths containing 0.1, 0.2, and 0.3 mmol dm^{-3} OT. The image a shows separated white islands whose height was estimated to be 0.25 nm on average from its cross-sectional profile as given in

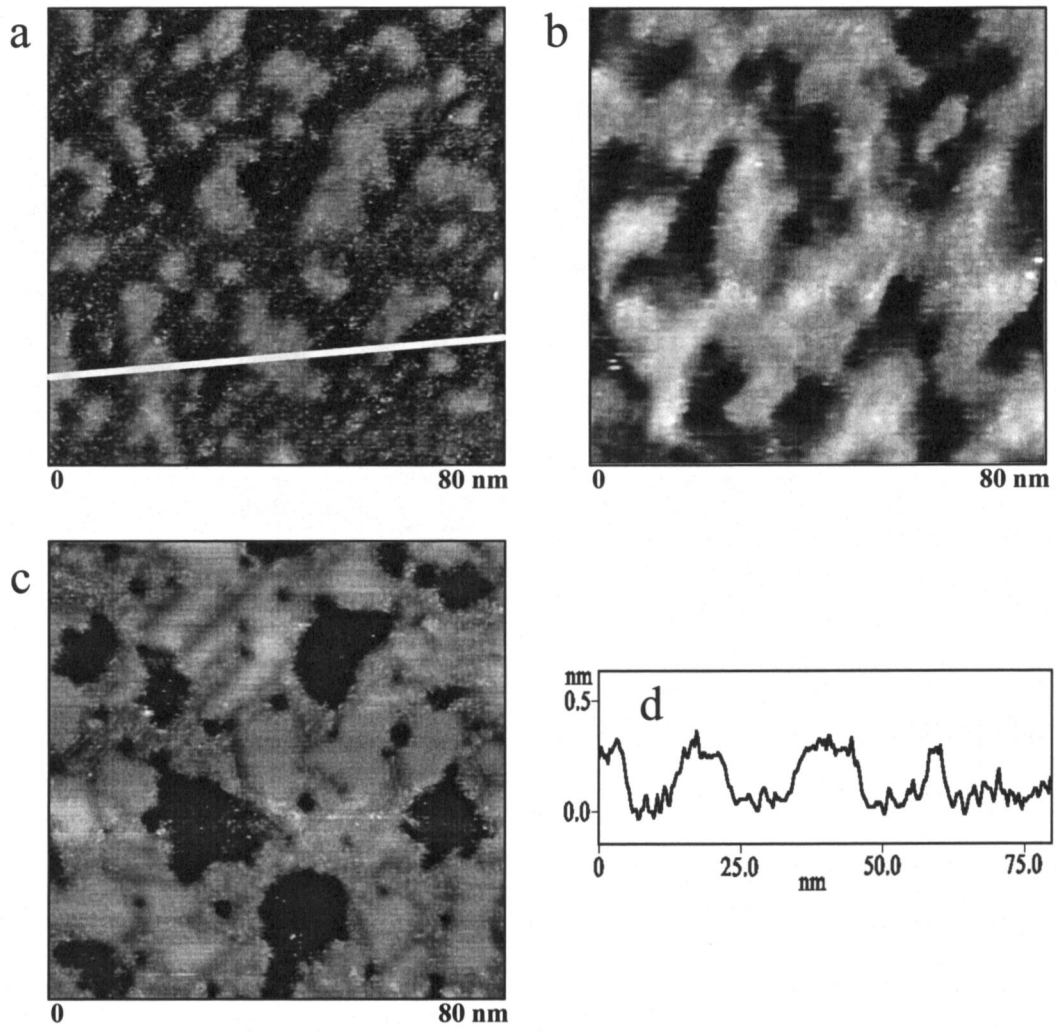

Figure 4-6. STM images of OT-MPA|Au electrode surfaces in 80 nm-squares taken after subjecting to the selective desorption of MPA by polarizing at –0.60 V vs. Ag|AgCl in 0.5 mol dm^{-3} KOH. The electrodes were prepared from the immersion baths containing 1 mmol dm^{-3} MPA and (a) 0.1, (b) 0.2, and (c) 0.3 mmol dm^{-3} OT. Cross-sectional profile (d) along the line drawn on the STM image (a).

Figure 4-6d. The higher resolution image of an island surface of 10 nm-square as shown in Figure 4-7 reveals hexagonally arrayed OT molecules with the shortest distance of 0.50 $\pm$ 0.04 nm, which is the value expected for the alkanethiol SAM having ($\sqrt{3}$ x $\sqrt{3}$)R30° structure. The height of islands mentioned above was much smaller than the value expected form the actual size of OT molecules adsorbed on an Au surface with a tilt angle of 30°. It has been, however, reported that the height of thiol molecules estimated by STM images tends to be much less than the value expected from the van der Waals length because of minimal contribution of the insulating organic layer to changes in the tunneling current of STM measurements.[108]

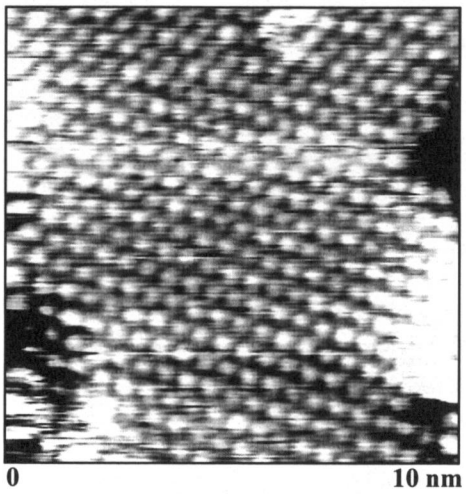

Figure 4-7. High resolution STM image of 10 nm-square surface of an OT island observed in the STM image shown in Figure 6a.

Comparison of three STM images shown in Figure 4-6 also reveals that the ratio of the areas of OT domains increased with increasing the OT concentration in the bath used for preparation of the electrode. It is noteworthy that as the OT-adsorbed areas becomes larger, the domains are attached to each other, giving a widely continuous domain. In the case of the electrode prepared from the solution containing 0.3 mmol dm^{-3} OT, round holes are present in the OT-SAM as shown in the image c, implying that the adsorbed MPA molecules have formed round domains in the binary OT-MPA SAMs.

The ratios of the OT-adsorbed areas were estimated from the STM images by using a Nanoscope III software, and the obtained values are also indicated by solid circles in Figure 4-5. The values obtained for DT-MPA, DDT-MPA, and HDT-MPA are also given in the same figure. Apparently, the occupation ratios of the long thiols obtained from the STM images are well accordance with the electrochemically evaluated mole fractions of the long thiols, suggesting that the STM images reflect directly surface aspects of the electrodes that was used for the voltammetry experiments.

Figure 4-8 shows STM images of the binary SAMs of DT-MPA, DDT-MPA, and HDT-MPA. The selective desorption of MPA was performed before STM observations for all cases to obtain higher contrast images. The baths used for the preparation of the DT-MPA and DDT-MPA SAMs contained 0.3 mmol dm^{-3} long thiol. However, since HDT molecules occupied almost all area in the HDT-MPA|Au electrode prepared from the solution containing 0.3 mmol dm^{-3} HDT, as shown in Figure 4-5, the shape of HDT and MPA domains could not be distinguished. Then, the surface of the electrode prepared using the immersion bath containing 0.1 mmol dm^{-3} HDT was given as the image c in Figure 4-8. In this case, the ratio of the HDT-adsorbed areas was comparable to those of other binary SAMs, as recognized from the results shown in Figure 4-5. The STM image of the DT-MPA SAMs shows presence of separated holes, indicating that the MPA in this binary SAMs also formed isolated domains. However, their shapes were more angular than the holes observed in the OT-MPA SAMs (see Figure 4-6c). In the cases of DDT-MPA and HDT-MPA SAMs, the MPA-adsorbed areas made bent wires or rather the long thiol molecules tended to make separated domains, as their chain lengths became longer. Similar images were usually obtained for the binary SAMs composed of thiols having large different lengths.[57,58,61,105-107]

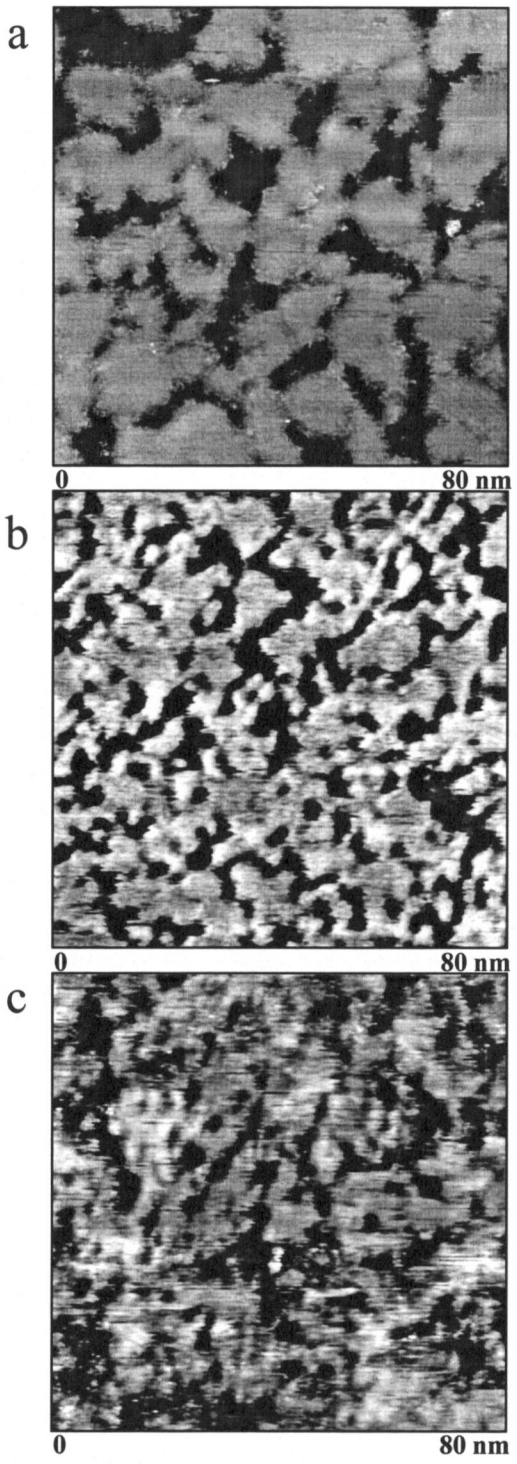

Figure 4-8. STM images of (a) DT-MPA|Au, (b) DDT-MPA|Au, and (c) HDT-MPA|Au electrodes in 80 nm-squares taken after subjecting to the selective desorption of MPA. The electrodes were prepared from the immersion baths containing 1 mmol dm^{-3} MPA and each long thiol in 0.3 mmol dm^{-3} (a,b) or 0.1 mmol dm^{-3} (c).

In order to make semi-quantitative evaluation of shapes of the holes observed in the STM images, their areas (A) and circumferences (L) were measured and the ratio of L^2/A were obtained, as shown in Figure 4-9a. The value of this ratio is 4π (= ca. 12.6) for the perfect round and becomes large with increasing degree of deviation from the round. The ratios of the holes observed in the images show n in Figure 4-6c and Figure 4-8 were evaluated, and the values were plotted as a function of the length of the long thiols, as shown in Figure 4-9b. The average value and degree of dispersion becomes large with increasing the length of the long thiol, indicating that it becomes difficult for MPA to make round domains when the thiols surrounding the MPA SAM are longer.

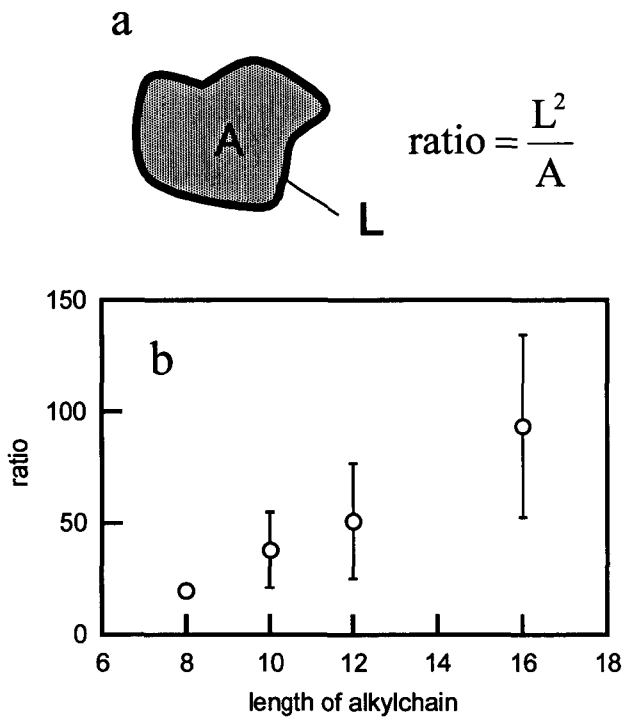

Figure 4-9. The ratio of square of circumference (L^2) to area (A) of a hole for evaluation of degree of deviation from the complete round, and (b) plots of the ratios obtained for shapes of MPA domains in the binary SAMs as a function of the alkylchain length of the long thiols.

Such variation in the spatial distribution of MPA and long thiol domains in the binary SAMs with changing the chain lengths of the long thiols seem to be explained by the difference in the molecular interactions inducing packed domains between the long thiol and MPA. When two impermissible liquids having comparable viscosity are mixed in different quantities, a liquid of small amount tends to make spherical trickles due to their surface tension originating from intermolecular affinities as the case of small amount of salad oil in water and vice versa. The variation in the distribution observed in the binary SAMs of OT-MPA as shown in Figure 4-6 seems to obey such natural rule. The molecular interaction of OT in its SAM must be larger than that of MPA, but their difference is not so different as compared with the combination of MPA and HDT. It is then likely that both thiols can keep their interaction for making separated round domains when the mole fraction becomes inferior in the binary SAMs. The same might be true for the DT-MPA binary SAMs as judged from the STM image shown in Figure 4-8a. However, when the chain length of the long thiol becomes longer, their molecular interaction is much larger than that of MPA, giving the situation that the molecular interaction of MPA is negligible. If this is true, the long thiols should keep a tendency to make separated domains regardless of their amount. Consequently, MPA is forcibly distributed around the long thiol domains like water being forcibly present around glutinous heavy oil.

4-4. Conclusions

The spatial distribution of long and short thiols in the binary SAMs is found to be influenced not only by their mole fractions but also by difference in degree of lengths between two thiols in this study. The binary SAMs are useful for arranging thiol molecules having specific functions on a metal surface.[14,16,20,107] Furthermore, the unique property of the binary SAMs should be ability to induce the selective desorption of the shorter thiol by electrochemical means. The resulting exposed area might be useful as electrochemically active surfaces[109] and templates for immobilizing substances including another thiol.[58,110] Then, the results obtained in

this study would give significant information for ones who would like to design the interface structures with use of the binary SAMs technique. However, although it has been evident in the present study that the distribution of the adsorbed thiol molecules in the binary SAMs can be controlled in some degree by choosing combination of the thiols, the method is not perfect for controlling completely the shapes of the thiol domains. To achieve such final goal, it is probably required to use other thiols having specific terminal groups that contribute the interactions of the adsorbed thiol molecules such as hydrogen bonds and electrostatic interactions. The investigation is still underway to elucidate how such interactions influence the distribution of thiols on the Au surface.

Summary

This thesis has dealt with elucidation of electrochemical properties of a self-assembled monolayer (SAM) of alkanethiols on an Au(111) surface, focusing on the effect of terminal groups and electrolyte ions on desorption behavior of SAMs. Then, their application for electrochemical methods to evaluate specific properties induced by self-assembly and to fabricate controlled nano-structures on electrode surfaces has been developed. The main results and conclusions obtained in this study are summarized as follows:

In chapter 1, SAMs of alkanethiols having various terminal groups on their ω-positions were formed on Au(111) electrodes and their reductive desorption is studied by linear sweep voltammetry, focusing on effects of solution pH on the desorption behavior. The peak potentials (E_p) of cathodic waves representing reductive desorption were found to be reflected by pK_a value of thiol group and were negatively shifted with an increase in pH of the electrolyte solution. The magnitude of pH dependency of E_p was greatly influenced by hydrophobicity of terminal groups. In the cases of alkanethiol SAMs having pH sensitive terminal groups such as carboxyl and amino groups, acidity of those groups was estimated from bending points appearing in the pH titration profile of E_p. This method allows direct determination of not only pK_a value of the arrayed groups but also that of the groups dissolved in solution simultaneously. The pK_a values of the arrayed carboxyl groups in SAMs were larger by ca. 3 pH units than their original ones, while those for amino groups were smaller by ca. 2 pH units.

In chapter 2, reductive desorption of alkanethiol-SAMs on Au(111) was investigated in ionic liquids. The E_p of reduction wave gives significant information concerning affinities between ions and functional groups substituted the terminals of alkanethiols. In ionic liquids, properties of not only cations but also anions influence the desorption behavior of SAMs.

In chapter 3, novel electrochemical methods to evaluate dynamic parameters of lipid membrane have been developed. Linear sweep voltammetry of the bilayer membrane-coated electrode shows reduction wave due to desorption of alkanethiol molecules. It was found that the peak potential of the reduction wave gave information concerning fluidity of the lipid layer. The electrochemical AC impedance measurements were found to be also useful for monitoring formation of the bilayer. There is no other method allowing kinetic studies on a planar bilayer membrane, the electrochemical methods developed in this study have high potential allowing to elucidate kinetic parameters that have never been obtained. Simplicity of the measurement instruments including the electrochemical cell is another merit and it allows combination of these measurements with another measurements.

In chapter 4, binary SAMs composed of 3-mercaptopropionic acid (MPA) and another alkanethiol that is longer than MPA were prepared by their coadsorption on an Au(111) electrode. Electrochemical measurements of the binary SAMs-coated Au electrodes revealed that selective desorption of MPA from the prepared binary SAMs can be induced by polarizing of the electrodes at –0.6 V vs. Ag/AgCl in 0.5 mol dm^{-3} KOH aqueous solution. STM observation of the electrode surfaces after subjecting to the selective desorption of MPA gave clear images showing spatial distribution of the long thiols in the binary SAMs, and it was revealed that the spatial distribution is influenced not only by their mole fractions but also by difference in degree of lengths between two thiols. The resulting exposed area might be useful as electrochemically active surfaces and templates for immobilizing substances including another thiol. Then, the results obtained in this study would give significant information for ones who would like to design the interface structures with use of the binary SAMs technique.

List of Publications

The content of the present thesis is composed of the following papers:

1. Spatial distribution of domains in binary self-assembled monolayers of thiols having different lengths
   Hirokazu Munakata, Susumu Kuwabata, Yoshihisa Ohko, and Hiroshi Yoneyama
   Journal of Electroanalytical Chemistry **2001**, *496*, 29–36

2. Detection of difference in acidity between arrayed carboxy groups and the groups dissolved in solution by reductive desorption of a self-assembled monolayer of carboxy-terminated thiols
   Hirokazu Munakata, and Susumu Kuwabata
   Chem. Commun. **2001**, 1338–1339

3. Development of Electrochemical Methods to Elucidate Dynamic Parameters of Lipid Molecules in Bilayer Membrane
   Susumu Kuwabata, Hirokazu Munakata, and Kyoko Watanabe
   Electrochemistry, **2003**, *71*, 933-937

4. Effect of ω-Functional Groups on pH-Depended Reductive Desorption of Alkanethiol Self-Assembled Monolayers
   Hirokazu Munakata, and Susumu Kuwabata
   Langmuir, in contribution

5. Voltammetric characterization of interfacial properties between alkanethiol self-assembled monolayers and ionic liquid
   Hirokazu Munakata, Yoshihiro Shibutani, and Susumu Kuwabata
   in preparation

Acknowledgement

First of all, I would like to express my great acknowledgment to Professor Dr. Susumu Kuwabata at Department of Materials Chemistry, Graduate School of Engineering, Osaka University for his continuous guidance, many invaluable suggestions, and his sincere encouragement throughout the course of this work.

I am also grateful to Professor Dr. Hiroshi Yoneyama (Anan College of Technology) and Professor Dr. Yasushi Kai for their helpful comments and suggestions.

I express my gratitude to Associate Professor Dr. Tsukasa Torimoto (Hokkaido University) and Assistant Professor Dr. Yoshihisa Ohko (Tokyo University) for many useful suggestions for performing experiments when they were in Osaka University.

I am obliged to Associate Professor Dr. Araki Masuyama, Assistant Professor Dr. Yasuhiro Tachibana, and Assistant Professor Dr. Daisuke Oyamatsu for stimulating discussions.

I appreciate all members of Electrochemistry Laboratory, especially my co-workers, Mr. Yoshihiro Shibutani and Ms. Kyoko Watanabe whose efforts enabled to progress this study.

Finally, I would like to express my deepest gratitude to my parents, Yutaka Munakata and Michiko Munakata, and my younger brother, Koji Munakata for giving me opportunity of pursuing this work and their perpetual supports.

Hirokazu Munakata

References

(1) Nuzzo, R. G.; Allara, D. L. *J. Am. Chem. Soc.* **1983**, *105*, 4481.

(2) Blodgett, K. B. *J. Am. Chem. Soc.* **1935**, *57*, 1007.

(3) Blodgett, K. B.; Langmuir, I. *Phys. Rev.* **1937**, *51*, 964.

(4) Dubois, L. H.; Nuzzo, R. G. *Annu. Rev. Phys. Chem.* **1992**, *43*, 437.

(5) Finklea, H. O. In *Electroanalytical Chemistry*; Bard, A. J., Rubinstein, I., Eds.; Marcel Dekker: New York, 1996; Vol. 19, pp 109-335.

(6) Ulman, A. *Chem. Rev.* **1996**, *96*, 1533.

(7) Bain, C. D.; Troughton, E. B.; Tao, Y. T.; Evall, J.; Whitesides, G. M.; Nuzzo, R. G. *J. Am. Chem. Soc.* **1989**, *111*, 321.

(8) Bain, C. D.; Whitesides, G. M. *Angew. Chem. Int. Ed. Engl.* **1989**, *28*, 506.

(9) Whitesides, G. M.; Laibinis, P. E. *Langmuir* **1990**, *6*, 87.

(10) Laibinis, P. E.; Fox, M. A.; Folkers, J. P.; Whitesides, G. M. *Langmuir* **1991**, *7*, 3167.

(11) Bain, C. D.; Whitesides, G. M. *J. Am. Chem. Soc.* **1988**, *110*, 3665.

(12) Laibinis, P. E.; Whitesides, G. M. *J. Am. Chem. Soc.* **1992**, *114*, 1990.

(13) Zamborini, F. P.; Crooks, R. M. *Langmuir* **1998**, *14*, 3279.

(14) Chidesy, C. E. D.; Loiacono, D. N. *Langmuir* **1990**, *6*, 682.

(15) Evans, S. D.; Sharma, R.; Ulman, A. *Langmuir* **1991**, *7*, 156.

(16) Rowe, G. K.; Creager, S. E. *Langmuir* **1991**, *7*, 2307.

(17) Ulman, A.; Evans, S. D.; Shnidman, Y.; Sharma, R.; Eilers, J. E.; Chang, J. C. *J. Am. Chem. Soc.* **1991**, *113*, 1499.

(18) Chailapakul, O.; Crooks, R. M. *Langmuir* **1993**, *9*, 884.

(19) Offord, D. A.; John, C. M.; Griffin, J. H. *Langmuir* **1994**, *10*, 761.

(20) Rowe, G. K.; Creager, S. E. *Langmuir* **1994**, *10*, 1186.

(21) Creager, S. E.; Clarke, J. *Langmuir* **1994**, *10*, 3675.

(22) Atre, S. V.; Liedberg, B.; Allara, D. L. *Langmuir* **1995**, *11*, 3882.

(23) Wilbur, J. L.; Biebuyck, H. A.; MacDonald, J. C.; Whitesides, G. M. *Langmuir* **1995**, *11*, 825.

(24) Kang, J. F.; Liao, S.; Jordan, R.; Ulman, A. *J. Am. Chem. Soc.* **1998**, *120*, 9662.

(25) Lahiri, J.; Ostuni, E.; Whitesides, G. M. *Langmuir* **1999**, *15*, 2055.

(26) Bain, C. D.; Whitesides, G. M. *J. Am. Chem. Soc.* **1988**, *110*, 6560.

(27) Bain, C. D.; Biebuyck, H. A.; Whitesides, G. M. *Langmuir* **1989**, *5*, 723.

(28) Bain, C. D.; Whitesides, G. M. *Langmuir* **1989**, *5*, 1370.

(29) Pale-Grosdemange, C.; Simon, E. S.; Prime, K. L.; Whitesides, G. M. *J. Am. Chem. Soc.* **1991**, *113*, 12.

(30) Folkers, J. P.; Laibinis, P. E.; Whitesides, G. M. *Langmuir* **1992**, *8*, 1330.

(31) Laibinis, P. E.; Nuzzo, R. G.; Whitesides, G. M. *J. Phys. Chem.* **1992**, *96*, 5097.

(32) Biebuyck, H. A.; Whitesides, G. M. *Langmuir* **1993**, *9*, 1766.

(33) Folkers, J. P.; Laibinis, P. E.; Whitesides, G. M.; Deutch, J. *J. Phys. Chem.* **1994**, *98*, 563.

(34) Wang, J.; Frostman, L. M.; Ward, M. D. *J. Phys. Chem.* **1992**, *96*, 5224.

(35) Shimazu, K.; Teranishi, T.; Sugihara, K.; Uosaki, K. *Chem. Lett.* **1998**, 669.

(36) Sugihara, K.; Teranishi, T.; Shimazu, K.; Uosaki, K. *Electrochemistry* **1999**, *67*, 1172.

(37) Sugihara, K.; Shimazu, K.; Uosaki, K. *Langmuir* **2000**, *16*, 7101.

(38) Guckenberger, R.; Heim, M.; Cevc, G.; Knapp, H. F.; Wiegraebe, W.; Hillebrand, A. *Science* **1994**, *266*.

(39) Delamarche, E.; Michel, B.; Biebuyck, H. A.; Gerber, C. *Adv. Mater.* **1996**, *8*, 719.

(40) Widrig, C. A.; Chung, C.; Porter, M. D. *J. Electroanal. Chem.* **1991**, *310*, 335.

(41) Walczak, M. M.; Pnpenoe, D. D.; Deinhammer, R. S.; Lamp, B. D.; Chung, C.; Porter, M. D. *Langmuir* **1991**, *7*, 2687.

(42) Vander, F. v. V. *Trans. Faraday Soc.* **1961**, *57*, 2263.

(43) Vander, F. v. V. *Trans. Faraday Soc.* **1963**, *59*, 1225.

(44) Tokiwa, F.; Ohki, K. *J. Phys. Chem.* **1967**, *71*, 1824.

(45) Bain, C. D.; Whitesides, G. M. *J. Am. Chem. Soc.* **1989**, *111*, 7164.

(46) Bain, C. D.; Evall, J.; Whitesides, G. M. *J. Am. Chem. Soc.* **1989**, *111*, 7155.

(47) Bryant, M. A.; Crooks, R. M. *Langmuir* **1993**, *9*, 385.

(48) Aoki, K.; Kakiuchi, T. *J. Electroanal. Chem.* **1999**, *478*, 101.

(49) Kakiuchi, T.; Iida, M.; Imabayashi, S.; Niki, K. *Langmuir* **2000**, *16*, 5397.

(50) Hu, K.; Bard, A. J. *Langmuir* **1997**, *13*, 5114.

(51) Van der Vegte, E. W.; Hadziioannou, G. *J. Phys. Chem. B* **1997**, *101*, 9563.

(52) Vezenov, D. V.; Noy, A.; Rozsnyai, L. F.; Lieber, C. M. *J. Am. Chem. Soc.* **1997**, *119*, 2006.

(53) Wallwork, M. L.; Smith, D. A.; Zhang, J.; Kirkham, J.; Robinson, C. *Langmuir* **2001**, *17*, 1126.

(54) Rodriguez, J. F.; Mebrahtu, T.; Soriaga, M. P. *J. Electroanal. Chem.* **1987**, *233*, 283-289.

(55) Walczak, M. M.; Alves, C. A.; Lamp, B. D.; Porter, M. D. *J. Electroanal. Chem.* **1995**, *396*, 103.

(56) Oyamatsu, D.; Nishizawa, M.; Kuwabata, S.; Yoneyama, H. *Langmuir* **1998**, *14*, 3298.

(57) Hobara, D.; Ota, M.; Imabayashi, S.; Niki, K.; Kakiuchi, T. *J. Electroanal. Chem.* **1998**, *444*, 113.

(58) Hobara, D.; Sasaki, T.; Imabayashi, S.; Kakiuchi, T. *Langmuir* **1999**, *15*, 5073.

(59) Imabayashi, S.; Iida, M.; Hobara, D.; Feng, Z. Q.; Niki, K.; Kakiuchi, T. *J. Electroanal. Chem.* **1997**, *428*, 33.

(60) Jencks, W. P.; Regenstein, J., In Handbook of Biochemistry and Molecular Biology; Fasman, G. D., Ed.; CRC Press: Cleveland, 1976; vol. 3, pp 305-351.

(61) Yang, D. F.; Wilde, C. P.; Morin, M. *Langmuir* **1996**, *12*, 6570.

(62) Zhong, C. J.; Porter, M. D. *J. Electroanal. Chem.* **1997**, *425*, 147.

(63) Byloos, M.; Al-Maznai, H.; Morin, M. *J. Phys. Chem. B* **1999**, *103*, 6554.

(64) Hurley, F. H.; Wier Jr., T. P. *J. Electrochem. Soc.* **1951**, *98*, 203.

(65) Wilkes, J. S.; Zaworotko, M. J. *J. Chem. Soc. Che. Commun.* **1992**, 965.

(66) Koch, V. R.; Nanjundiah, C.; Appecchi, G. B.; Scrosati, B. *J. Electrochem. Soc.* **1995**, *142*, L116.

(67) Holbery, J. D.; Seddon, K. R. *J. Chem. Soc., Dalton Trans.* **1999**, 2133.

(68) Welton, T. *Chem. Rev.* **1999**, *99*, 2071.

(69) Wilkes, J. S.; Levisky, J. A.; Wilson, R. A.; Hussey, C. L. *Inorg. Chem.* **1982**, *21*, 1263.

(70) Nanjundiah, C.; McDevitt, S. F.; Koch, V. R. *J. Electrochem. Soc.* **1997**, *144*, 3392.

(71) Noda, A.; Hayamizu, K.; Watanabe, M. *J. phys. Chem. B* **2001**, *105*, 4603.

(72) Bangham, A. D.; Standish, M. M.; Watkins, J. C. *J. Mol. Biol.* **1965**, *13*, 238.

(73) Chapman, D.; Owens, N. F.; Walker, J. C. *Biochim. Biophys. Acta* **1966**, *120*, 148.

(74) Damel, R. A.; van Deenen, L. L. M.; Pethica, B. A. *Biochim. Biophys. Acta* **1967**, *135*, 11.

(75) Reiss-Husson, F. *J. Mol. Biol.* **1967**, *25*, 363.

(76) Papahadjopoulos, D.; Weiss, L. *Biochim. Biophys. Acta* **1969**, *138*, 417.

(77) Singer, S. J.; Nicolson, G. R. *Science* **1972**, *175*, 720.

(78) Imai, M.; Inoue, K.; Nojima, S. *Biochim. Biophys. Acta* **1975**, *375*, 130.

(79) Szoka, F. C.; Papahadjopoulos, D. *Ann. Rev. Biophys. Bioeng.* **1980**, *9*, 467.

(80) Lichtenberg, D.; Barenholz, Y. *Meth. Biochem. Anal.* **1988**, *33*, 337.

(81) Fleischer, S.; Fleischer, B. *Meth. Enzymol.* **1989**, *171*, 191.

(82) Tien, H. T.; Howard, R. E. In *Techniques of Surface and Colloid Chemistry and Physics*; Good, R. J., Stromberg, R. R., Patrick, R. L., Eds.; Marcel Dekker: NY, 1972, p 109.

(83) Tien, H. T. *J. Phys. Chem.* **1984**, *88*, 3172.

(84) Gu, L. Q.; Wang, L. G.; Xun, J.; Ottova, A. L.; Tien, H. T. *Bioelectrochem. Bioeng.* **1996**, *39*, 275.

(85) Tien, H. T.; Wurster, S. H.; Ottova, A. L. *Bioelectrochem. Bioeng.* **1997**, *42*, 77.

(86) Struck, D. K.; Hoekstra, D.; Pagano, R. E. *Biochemistry* **1981**, *20*, 4093.

(87) Hoekstra, D. *Biochemistry* **1982**, *21*, 2833.

(88) Ottova, A. L.; Tien, H. T. *Prog. Surf. Sci.* **1992**, *41*, 337.

(89) Ottova, A. L.; Martynski, T.; Wardak, A.; Tien, H. T. In *Adv. Chem. Series No. 240*; Birge, R., Ed.; American Chemical Society: Washington, 1994, p 439.

(90) Naumann, R.; Jonczyk, A.; Kopp, R.; van Esch, J.; Ringsdorf, H.; Koll, W.; Graber, P. *Angew. Chem. Int. Ed. Engl.* **1995**, *34*, 2056.

(91) Lu, X. D.; Ottova, A. L.; Tien, H. T. *Bioelectrochem. Bioeng.* **1996**, *39*, 285.

(92) Yuan, H. P.; Ottova, A. L.; Tien, H. T. *Mat. Scie. Eng. C* **1996**, *4*, 35.

(93) Cornell, B. A.; Braach-Maksvytis, V. L. B.; King, L. G.; Osman, D. J.; Raguse, B.; Wieczorek, L.; Pace, R. J. *Nature* **1997**, *387*, 580.

(94) Plant, A. L. *Langmuir* **1993**, *9*, 2764.

(95) Plant, A. L.; Gueguetchkeri, M.; Yap, W. *Biophys. J.* **1994**, *67*, 1126.

(96) Ding, L.; Li, J.; Wang, E.; Dong, S. *Thin Solid Films* **1997**, *293*, 153.

(97) Nakaminami, T.; Ito, S.; Kuwabata, S.; Yoneyama, H. *Anal. Chem.* **1999**, *71*, 4278.

(98) Oyamatsu, D.; Kuwabata, S.; Yoneyama, H. *J. Electroanal. Chem.* **1999**, *473*, 59.

(99) Hobara, D.; Miyake, S.; Niki, K.; Kakiuchi, T. *Langmuir* **1998**, *14*, 3590.

(100) Aoki, K.; Kakiuchi, T. *J. Electroanal. Chem.* **1998**, *452*, 187.

(101) Landbrooke, B. D.; Williams, R. M.; Chapman, D. *Biochim. Biophys. Acta* **1968**, *150*, 333.

(102) Demel, R. A.; Geurts van Kessel, W. S. M.; van Deenen, L. L. M. *Biochim. Biophys. Acta* **1972**, *266*, 26.

(103) de Gier, J.; Mandersloot, J. G.; van Deenen, L. L. M. *Biochim. Biophys. Acta* **1969**, *173*, 143.

(104) Ganapathi, R.; Keishan, A. *Biochim. Pharmacol.* **1984**, *39*, 698.

(105) Takami, T.; Delamarche, E.; Michel, B.; Gerber, C.; Wolf, H.; Ringsdorf, H. *Langmuir* **1995**, *11*, 3876.

(106) Stranick, S. J.; Parikh, A. N.; Tao, Y. T.; Allara, D. L.; Weiss, P. S. *J. Phys. Chem.* **1994**, *98*, 7636.

(107) Sato, Y.; Yamada, R.; Mizutani, F.; Uosaki, K. *Chem. Lett.* **1997**, 987.

(108) Poirier, G. E.; Pylant, E. D. *Science* **1996**, *272*, 1145.

(109) Nishizawa, M.; Sunagawa, T.; Yoneyama, H. *J. Electroanal. Chem.* **1997**, *436*, 213.

(110) Imabayashi, S.; Hobara, D.; Kakiuchi, T.; Knoll, W. *Langmuir* **1997**, *13*, 4502.